Atmos. Chem. Phys. Discuss., doi:10.5194/acp-2016-1163, 2017
Manuscript under review for journal Atmos. Chem. Phys.
Discussion started: 2 March 2017

Atmospheric Chemistry and Physics Discussions

CCl_4 distribution derived from MIPAS ESA V7 data: validation, trend and lifetime estimation

Massimo Valeri[1,2], Flavio Barbara[3], Chris Boone[4], Simone Ceccherini[3], Marco Gai[3], Guido Maucher[6], Piera Raspollini[3], Marco Ridolfi[1,3], Luca Sgheri[5], Gerald Wetzel[6], and Nicola Zoppetti[3]

[1]Dipartimento di Fisica e Astronomia, Università di Bologna, Italy
[2]Istituto di Scienze dell'Atmosfera e del Clima, Consiglio Nazionale delle Ricerche, Bologna, Italy
[3]Istituto di Fisica Applicata "Carrara", Consiglio Nazionale delle Ricerche, Firenze, Italy
[4]Department of Chemistry, University of Waterloo, Waterloo, Ontario, Canada
[5]Istituto per le Applicazioni del Calcolo, Consiglio Nazionale delle Ricerche, Firenze, Italy
[6]Karlsruhe Institute of Technology, Institute of Meteorology and Climate Research, Karlsruhe, Germany

Correspondence to: Marco Ridolfi (marco.ridolfi@unibo.it)

Abstract. Atmospheric emissions of Carbon tetrachloride (CCl_4) are regulated by the Montreal Protocol due to its role as a strong ozone-depleting substance. The molecule has been the subject of recent increased interest as a consequence of the so called "mystery of CCl_4," the discrepancy between atmospheric observations and reported production and consumption. Surface measurements of CCl_4 atmospheric concentrations have declined at a rate almost three times smaller than its lifetime-limited rate, suggesting persistent atmospheric emissions despite the ban. In this paper, we study CCl_4 vertical and zonal distributions in the upper troposphere and lower stratosphere (including the photolytic loss region, 70-20 hPa), its trend, and its stratospheric lifetime using measurements from the Michelson Interferometer for Passive Atmospheric Sounding (MIPAS), which operated onboard the ENVISAT satellite from 2002 to 2012. Specifically, we use the MIPAS data product generated with Version 7 of the Level 2 algorithm operated by the European Space Agency.

The CCl_4 zonal means show features typical of long-lived species of anthropogenic origin that are destroyed primarily in the stratosphere, with larger quantities in the troposphere and a monotonic decrease with increasing altitude in the stratosphere. In the troposphere, the largest concentrations are observed at the latitudes of major industrial countries (20°/50°N). The good agreement we find between MIPAS CCl_4 and independent measurements from other satellite and balloon-borne remote sounders proves the reliability of the MIPAS dataset.

CCl_4 trends are calculated as a function of both latitude and altitude. Negative trends are found at all latitudes in the upper-troposphere / lower-stratosphere region, apart from a region in the Southern mid-latitudes between 50 and 10 hPa where the trend is positive. At the lowest altitudes sounded by MIPAS, we find trends consistent with those determined on the basis of long-term ground-based measurements. For higher altitudes, the trend shows a pronounced asymmetry between Northern and Southern Hemispheres, and the magnitude of the decline rate increases with altitude. At 50 hPa the decline is about 30-35%/decade, close to the lifetime-limited trend.

Atmos. Chem. Phys. Discuss., doi:10.5194/acp-2016-1163, 2017
Manuscript under review for journal Atmos. Chem. Phys.
Discussion started: 2 March 2017

Atmospheric Chemistry and Physics Discussions

We use a simplified model assuming tracer-tracer linear correlations to determine CCl_4 lifetime in the lower stratosphere. The calculation provides a global average lifetime of 46(38 - 60) years considering CFC-11 as the reference tracer. This value is consistent with the most recent literature result of 44(36 - 58) years.

1 Introduction

Carbon tetrachloride (CCl_4) is a strong ozone-depleting substance with an ozone depleting potential of 0.72 and a strong greenhouse gas with a 100-year global warming potential of 1730 (Harris et al., 2014). Regulated by the Montreal Protocol, the production of CCl_4 for dispersive applications was banned for developed countries in 1996, while developing countries were allowed a delayed reduction with the complete elimination by 2010 (Liang et al., 2014). CCl_4 can still be legally used as a feedstock, for example in the production of hydro-fluorocarbons.

The dominant loss mechanism for atmospheric CCl_4 is through photolysis in the stratosphere. The other major sinks are degradation in the oceans and degradation in soil. The estimated partial lifetimes provided in the latest ozone assessment report (Carpenter et al., 2014) with respect to these three sinks are 44 years for the atmospheric sink, 94 years for the oceanic sink, and 195 years for the soil sink. The combination of these three partial loss rates yields a total lifetime estimate of 26 years.

CCl_4 atmospheric concentration is routinely monitored by global networks such as Advanced Global Atmospheric Gases Experiment (AGAGE, http://agage.mit.edu/) (Simmonds et al., 1998; Prinn et al., 2000, 2016) and National Oceanic and Atmospheric Administration / Earth System Research Laboratory / Halocarbons & other Atmospheric Trace Species (NOAA / ESRL / HATS, http://www.esrl.noaa.gov/gmd/hats/). The concentration of CCl_4 has been decreasing in the atmosphere since the early 1990s, and the latest ozone assessment report (Carpenter et al., 2014) indicates that the global surface mean mole fraction of CCl_4 continued to decline from 2008 to 2012. AGAGE and University of California Irvine (UCI) networks report rates of decline of 1.2–1.3% yr^{-1} from 2011 to 2012, whereas the rate of decline reported by the NOAA/HATS network was 1.6% yr^{-1}. These relative declines in mole fractions at Earth's surface are comparable to declines in column abundances of 1.1–1.2% yr^{-1} (Brown et al., 2011; Rinsland et al., 2012).

A significant discrepancy is observed between global emissions estimates of CCl_4 derived by reported production and feedstock usage (bottom-up emissions) compared to those derived by atmospheric observations (top-down emissions). This discrepancy has recently stimulated a particular interest in furthering the understanding of atmospheric CCl_4. A study performed with a 3-D chemistry-climate model using the observed global trend and the observed inter-hemispheric gradient (1.5 ± 0.2 ppt for 2000–2012) estimated a total lifetime of 35 years (Liang et al., 2014). Recently, a study has reassessed the partial lifetime with respect to the soil sink to be 375 years (Rhew and Happell, 2016), and another study has reassessed the partial lifetime with respect to the ocean sink to be 209 years (Butler et al., 2016). These new estimates of the partial lifetimes with respect to soil and oceanic sinks produce a new total lifetime estimate of 33 years, consistent with the estimate given in Liang et al. (2014). This longer total lifetime reduces the discrepancy between the bottom-up and top-down emissions from 54 Gg yr^{-1} to 15 Gg yr^{-1} (SPARC, 2016). While the new bottom-up emission is still less than the top-down emission, the new estimates reconcile the CCl_4 budget discrepancy when considered at the edges of their uncertainties. A recent study estimated that the

Atmos. Chem. Phys. Discuss., doi:10.5194/acp-2016-1163, 2017
Manuscript under review for journal Atmos. Chem. Phys.
Discussion started: 2 March 2017

Atmospheric Chemistry and Physics Discussions

average European emissions for 2006–2014 were 2.3 Gg yr^{-1} (Graziosi et al., 2016), with an average decreasing trend of 7.3% per year.

Since the atmospheric loss of $\mathrm{CCl_4}$ is mainly due to photolysis in the stratosphere, satellite measurements that provide vertical profiles are particularly useful in validating the stratospheric loss rates in atmospheric models. A global distribution of $\mathrm{CCl_4}$ extending up to the mid-stratosphere was obtained by the Atmospheric Chemistry Experiment-Fourier Transform Spectrometer (ACE-FTS) (Allen et al., 2009). This study derived an atmospheric lifetime of 34 years through correlation with CFC-11. Another determination of the atmospheric lifetime of $\mathrm{CCl_4}$ was produced with ACE-FTS measurements in Brown et al. (2011), where the lifetime is estimated to be 35 years. A trend of atmospheric $\mathrm{CCl_4}$ from ACE-FTS measurements was reported in Brown et al. (2013), averaged in the 30° S/30° N latitude belt and in the altitude range from 5 to 17 km, were it was found to be decreasing at a rate of 1.2% yr^{-1}.

In this paper, we report the global atmospheric distribution of $\mathrm{CCl_4}$ as a function of altitude and latitude obtained from the measurements of the limb emission sounder MIPAS (Michelson Interferometer for Passive Atmospheric Sounding) (Fischer et al., 2008) onboard the ENVISAT satellite. The data product employed here was generated with the processor of the European Space Agency (ESA) Version 7 (ESA, 2016). MIPAS $\mathrm{CCl_4}$ vertical profiles are validated by comparing them with correlative independent measurements. The trend of $\mathrm{CCl_4}$ as a function of altitude and latitude is also determined. The MIPAS measurements provide a denser and more complete geographical coverage than those provided by the ACE-FTS measurements, allowing a more precise knowledge of the $\mathrm{CCl_4}$ global distribution and of the trend. The key photolytic loss region (70-20 hPa) is also analyzed.

In Section 2, we introduce MIPAS measurements, the retrieval setup, and the error budget of the $\mathrm{CCl_4}$ profiles. In Section 3, we discuss the global $\mathrm{CCl_4}$ distribution and the inter–hemispheric differences determined from MIPAS measurements. In Section 4, we show the results of the comparisons between MIPAS and $\mathrm{CCl_4}$ correlative measurements from the balloon version of the MIPAS instrument and the ACE-FTS. In Section 5, we illustrate the method adopted for the estimation of the atmospheric trends and the results of trend analysis, along with some comparisons to previously published results. In Section 6, we evaluate the $\mathrm{CCl_4}$ stratospheric lifetime using the tracer-tracer linear correlation method and compare the results with previously published estimates.

2 MIPAS measurements

In the first two years of operations (from July 2002 to March 2004) MIPAS acquired, nearly continuously, measurements at Full spectral Resolution (FR), with a spectral sampling of $0.025\ \mathrm{cm}^{-1}$. On 26 March 2004, FR measurements were interrupted due to an anomaly in the movement of the interferometer drive unit. After instrument diagnosis and tests by the hardware experts, atmospheric measurements were resumed in January 2005. After this date, however, MIPAS adopted a reduced spectral resolution of $0.0625\ \mathrm{cm}^{-1}$. Being achievable with a shorter interferometric scan, measurements with this spectral resolution require a reduced measurement time compared to the FR, thus allowing a finer spatial sampling. For this reason, the measurements acquired from January 2005 onward are referred to as Optimized Resolution (OR) measurements. Compared to the FR,

Atmos. Chem. Phys. Discuss., doi:10.5194/acp-2016-1163, 2017
Manuscript under review for journal Atmos. Chem. Phys.
Discussion started: 2 March 2017

Atmospheric Chemistry and Physics Discussions

they show both a reduced Noise Equivalent Spectral Radiance (NESR), and finer vertical and horizontal spatial samplings. The nominal FR (OR) scan pattern consists of 17 (27) sweeps with tangent heights in the range from 6-68 (7-72) km with 3 (1.5) km steps in the Upper Troposphere / Lower Stratosphere (UTLS) region. Full details of the MIPAS measurements acquired in the two mission phases are reported in Raspollini et al. (2013). It is worth mentioning here that in both mission phases MIPAS measurements cover the whole globe with a dense sampling, facilitating detailed studies on the evolution of atmospheric composition. The ESA operational Level 2 algorithm retrieves target parameters at the tangent points of the limb measurements (or at a subset of them). The inversion process minimizes the χ^2–function, using the Gauss-Newton iterative scheme with the Marquardt modification. An adaptive a-posteriori regularization is used in order to smooth the profiles with a strength determined on the basis of the error bars of the unregularized profile (Ceccherini, 2005; Ceccherini et al., 2007; Ridolfi and Sgheri, 2009, 2011). The ESA Level 2 processor version 7 retrieves CCl_4 volume mixing ratio (VMR) profiles simultaneously with a set of other target parameters. The retrieval is based on the fit of a set of narrow (3 cm^{-1}) spectral intervals called microwindows (MWs) containing relevant information on the target parameters. As for all MIPAS ESA retrievals, the MWs for CCl_4 retrievals are selected with the MWMAKE algorithm (Dudhia et al., 2002). This algorithm identifies the spectral intervals to be used in the inversion, with the aim of minimizing the total retrieval errors (including both systematic and random components). The MWs used in the ESA Level 2 retrievals from nominal FR and OR measurements are listed in Table 1.

CCl_4 VMR is retrieved only up to about 27 km, since above this altitude the CCl_4 concentration is too small to generate a sufficient contribution to the measured spectrum for analysis. Furthermore, to avoid numerical instabilities in the inversion of OR measurements (that vertically oversample the limb), the retrieval grid includes only one out of every two tangent points. Fig. 1 characterizes a typical CCl_4 retrieval from nominal limb scans acquired in the FR (top panel) and OR (bottom panel) measurement phases. The coloured solid lines show the 8 rows (corresponding to the 8 retrieval grid points) of the Averaging Kernels (AKs). Typically the number of degrees of freedom of the retrieval (trace of the AK matrix) is 5–6 for FR and 4–5 for OR measurements. The slightly smaller number of degrees of freedom obtained in the OR retrievals stems from the fact that, to make the retrieval more stable, CCl_4 is not retrieved at every tangent point of the OR limb measurements. The dotted red line of Fig. 1 represents the vertical resolution, calculated as the Full Width Half Maximum (FWHM) of the AK rows.

2.1 Error budget

To evaluate the CCl_4 VMR error due to the mapping of the measurement noise in the retrieval we use the error covariance matrix provided by the retrieval algorithm (Ceccherini and Ridolfi, 2010). The other error components affecting the individual CCl_4 VMR profiles are evaluated at Oxford University using the MWMAKE tool. Fig. 2 summarizes the most relevant error components affecting each individual retrieved CCl_4 profile, using the MWs of Table 1, for both the FR (top panel) and OR (bottom panel) nominal MIPAS measurement cases.

The key “RND” in the plots refers to the mapping of the measurement noise in the retrieval, as evaluated for typical FR and OR retrievals. Apart from the “NLGAIN” error that will be discussed later, the other error components, in both the FR and OR cases, can be grouped as follows: a) the errors due to the uncertainties in the (previously retrieved) pressure and temperature

Atmos. Chem. Phys. Discuss., doi:10.5194/acp-2016-1163, 2017
Manuscript under review for journal Atmos. Chem. Phys.
Discussion started: 2 March 2017

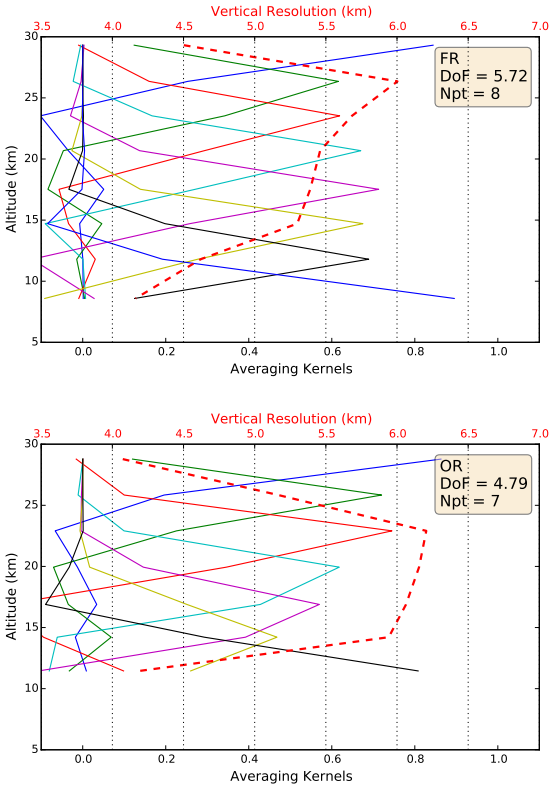

Figure 1. Typical AKs (coloured lines) and vertical resolution (red dotted lines) of CCl_4 VMR retrieved from FR (top) and OR (bottom) MIPAS measurements.

profiles (PT), and VMR of spectrally interfering gases, for example O_3, H_2O, HNO_3 and NH_3; b) the error due to horizontal variability of the atmosphere (GRAD) not included in the model; c) the uncertainties in the spectroscopic (SPECDB) and cross-section (LUT) databases and the error in the CO_2 line mixing model (CO2MIX); d) the errors due to less than perfect instrument line-shape characterization, namely its spectral shift (SHIFT) and width (SPREAD). For the details on how the different error components were calculated by MWMAKE, see Dudhia et al. (2002) and the Oxford University MIPAS website (Oxford University, 2016).

The main errors of type a) are due to interfering gases whose VMRs are retrieved before CCl_4 with some random error. Therefore, like the RND error component, they change randomly from profile to profile. Thus, in the calculated (monthly) averages they scale down with the inverse square root of the number of averaged profiles. The errors of type b), as shown

Atmos. Chem. Phys. Discuss., doi:10.5194/acp-2016-1163, 2017
Manuscript under review for journal Atmos. Chem. Phys.
Discussion started: 2 March 2017

Atmospheric Chemistry and Physics Discussions

MWs used in CCl_4 retrievals from FR measurements	
Start wavenumber cm^{-1}	End wavenumber cm^{-1}
796.3750	799.3750
800.2750	803.2750
792.7000	795.7000
771.8000	773.7750

MWs used in CCl_4 retrievals from OR measurements	
Start wavenumber cm^{-1}	End wavenumber cm^{-1}
792.8125	795.8125

Table 1. MW used for CCl_4 retrieval from nominal FR and OR MIPAS measurements.

in Castelli et al. (2016), cause systematic (and opposite in sign) differences between profiles retrieved from measurements acquired in the ascending and the descending parts of the satellite orbits. These errors cancel-out when calculating averages that evenly include profiles retrieved from measurements belonging to the ascending and the descending parts of the orbits. Errors of type c) are constant and may cause profile biases, however, being constant, they do not affect the calculated trends. Regarding the errors due to the imperfect instrument line-shape modeling (type d), since the gain of MIPAS bolometric detectors remained constant throughout the whole mission, there is no hint of a possible degradation of instrument optics and thus of a possible change in the instrument line-shape. This type of error, therefore, also has no impact in trend calculations.

Imperfect instrument radiometric calibration also causes an error. This error is plotted in Fig. 2 with the label "NLGAIN". Being of the order of 0.4% in the upper part of the retrieval range, it is rather small in individual CCl_4 profiles. Although small, this error is important when calculating atmospheric trends as it includes the uncertainty in the correction applied to the radiances to account for the non-linearities of MIPAS photometric detectors (Kleinert et al., 2007). In MIPAS Level 1b radiances up to version 5, the applied non-linearity correction is constant throughout the whole MIPAS mission. However, non-linearities change over the course of the mission due to progressive ageing of the detectors. A constant correction implies, therefore, a drift of the radiometric calibration error during the mission, with a direct impact in the calculated trends. MIPAS Level 1b radiances version 7 overcome this problem as they use a time-dependent non-linearity correction scheme. The residual drift of the calibration error after this time-dependent correction is still being characterized; however, preliminary results (Birk priv. com. 2016) show that it is smaller than 1% across the entire mission. MIPAS Level 1b radiances version 5 were used in the past to extract information on trends of different gases, either ignoring this effect (see, e.g., CFC-11/CFC-12 in Kellmann et al. (2012), or HCFC-22 in Chirkov et al. (2016)) or correcting the drift via intercomparison with other instruments assumed to be drift-free (Eckert et al., 2014). Recently it has been shown (Eckert et al., 2016) that ignoring this effect introduces a significant error on the trend estimation. The MIPAS Level 1b calibrated radiances version 7 employed here are considered a significant improvement from the point of view of the correction of this drift.

Atmos. Chem. Phys. Discuss., doi:10.5194/acp-2016-1163, 2017
Manuscript under review for journal Atmos. Chem. Phys.
Discussion started: 2 March 2017

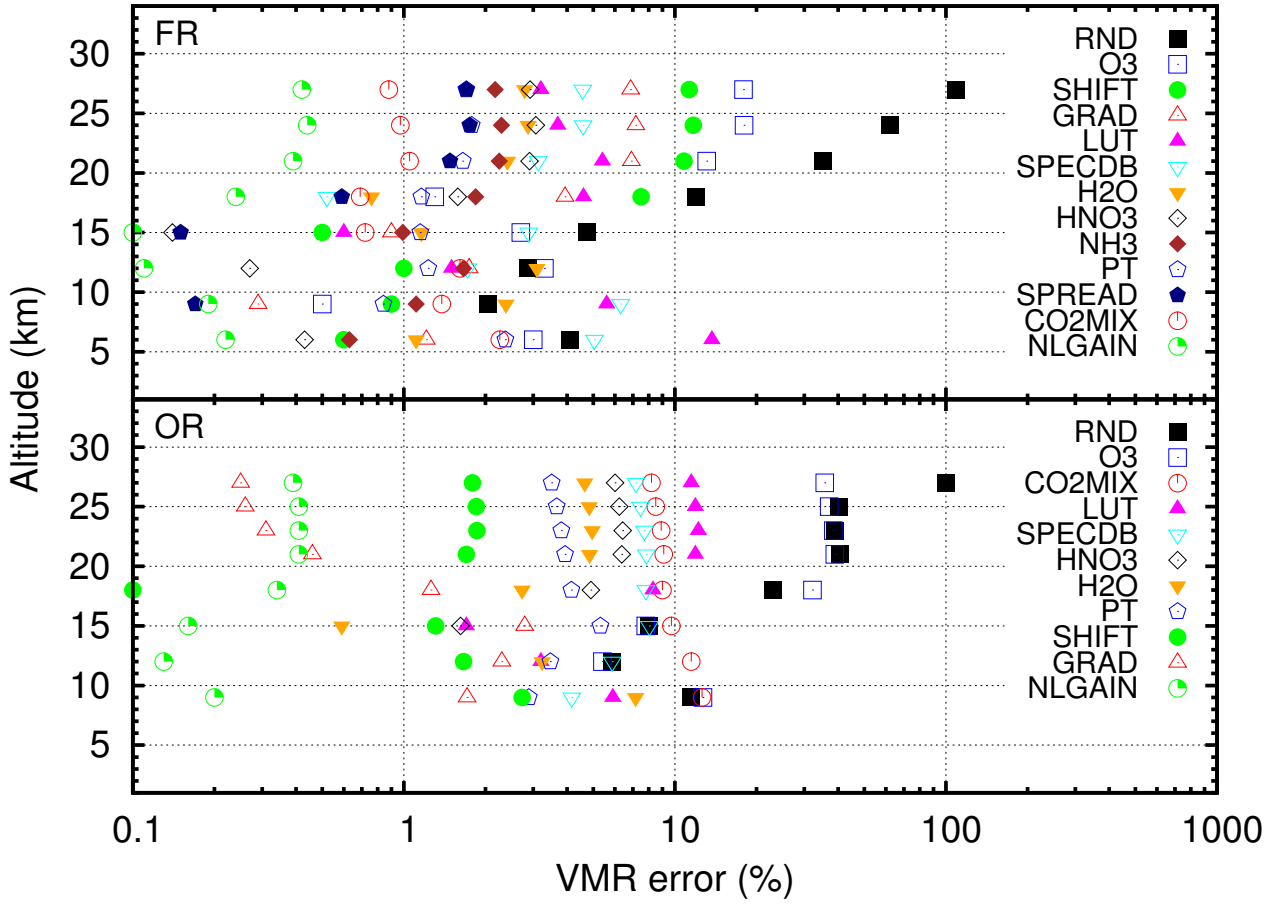

Figure 2. Main error components of the individual retrieved CCl_4 VMR profiles from FR (top) and OR (bottom) nominal MIPAS measurements.

The general good quality of fits obtained in CCl_4 retrievals is illustrated in Fig. 3. The figure refers to the MWs used in the FR retrievals. We are not showing the residuals in the single MW used for OR retrievals as it mostly overlaps the third MW of FR retrievals. The upper plot of Fig. 3 shows the average of 1141 observed (black dots) and simulated (red line) limb radiances in the MWs used for CCl_4 retrievals. The averages include spectra with tangent heights in the range from 6 to 17 km. The lower plot shows the average residuals of the fit (observation minus simulation, blue line) as well as the average noise level of the individual MIPAS measurements (dashed lines). The grey areas indicate spectral channels that, as recommended by the MWMAKE algorithm, are excluded from the fit to minimize the total retrieval error. Note that the average residuals shown in Fig. 3 have an associated random error given by the noise of the individual measured spectra divided by the square root of the number of averaged spectra, i.e. $\approx 1\mathrm{nW}/(\mathrm{cm}^2\mathrm{sr}\,\mathrm{cm}^{-1})$. This implies that while the amplitude of the average residuals is not

Atmos. Chem. Phys. Discuss., doi:10.5194/acp-2016-1163, 2017
Manuscript under review for journal Atmos. Chem. Phys.
Discussion started: 2 March 2017

Atmospheric Chemistry and Physics Discussions

compatible with their noise error, the additional systematic uncertainties are still smaller than the noise error of the individual measured spectra, in agreement with the predictions reported in Fig. 2.

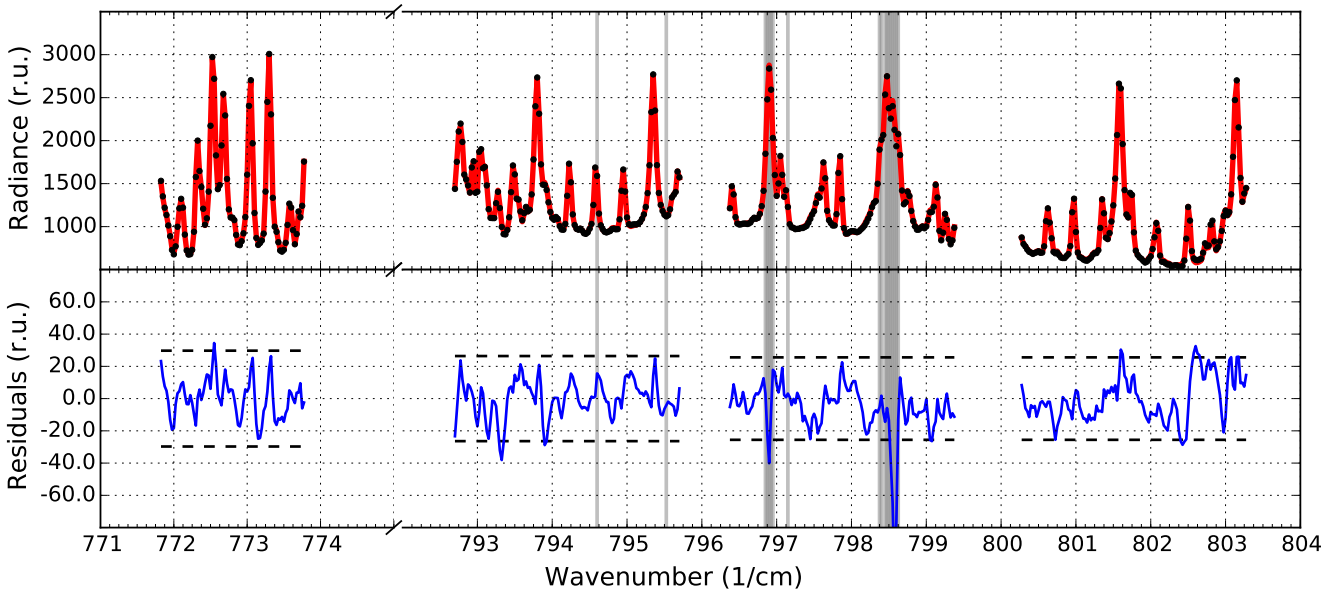

Figure 3. The upper plot shows an average of 1141 observed (black dots) and simulated (red line) limb radiances in the MWs used for CCl_4 FR retrievals. The averages include spectra with tangent height from 6 to 17 km.The lower plot shows the average residuals of the fit (blue line, observation minus simulation) as well as the average noise level of the individual measurements (dashed lines). The grey areas indicate spectral channels excluded from the fit. The radiance units (r.u.) in the vertical axes of the plots are $\mathrm{nW/(cm^2 sr\,cm^{-1})}$.

3 CCl_4 global distribution

Figure 4 shows the global monthly distribution of MIPAS CCl_4 VMR for a representative month from each of the four seasons, spanning the time period from August 2010 through May 2011. Here, retrieved profiles were first interpolated to fixed pressure levels (see Sect.5.1), and then binned in 5° latitude intervals. In all the considered months, the zonal averages show the typical shape of the long-lived species of anthropogenic origin, which are emitted at the surface and destroyed primarily in the stratosphere. Larger values are found in the troposphere, and then the VMR monotonically decreases with increasing altitude in the stratosphere. In the lower stratosphere, concentrations between 30° S and 30° N are significantly larger compared to those at higher latitudes. This pattern can be attributed to the Brewer-Dobson circulation that is responsible for the uplift of the surface air in the tropical regions. The CCl_4 distribution shows also a seasonal variability. The intrusion of CCl_4-poor mesospheric air in the stratosphere during winter, due to the air subsidence induced by the polar vortex, is clearly visible in both polar winters, its effects continuing into early spring and extending into the troposphere. Minimum CCl_4 values are observed in November in the South Pole and in March in the North Pole (November is considered the beginning of spring in the South Pole, whereas

Atmos. Chem. Phys. Discuss., doi:10.5194/acp-2016-1163, 2017
Manuscript under review for journal Atmos. Chem. Phys.
Discussion started: 2 March 2017

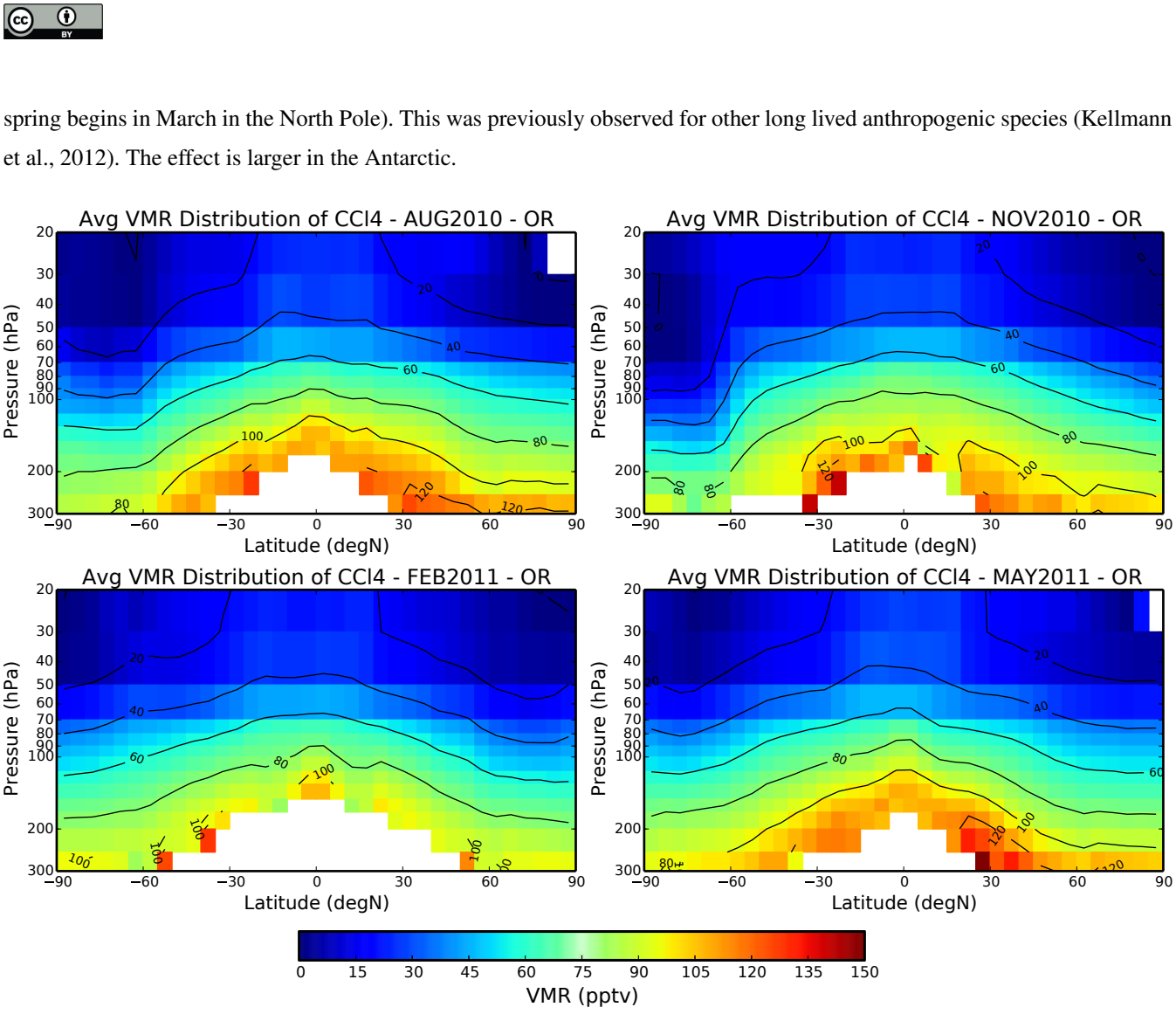

Figure 4. Zonal monthly averages of MIPAS CCl_4 profiles. The maps refer to four separate months in different seasons: August 2010 (top left), November 2010 (top right), February 2011 (bottom left) and May 20117 (bottom right).

The maps in Fig. 5 show the time evolution of CCl_4 at all latitudes from July 2002 to April 2012. The three maps refer to different pressure levels: 50 hPa (upper map), 90 hPa (middle map) and 130 hPa (lower map). The seasonal variability is also clearly visible from the maps of Fig. 4, with opposite phases in the two Hemispheres, more pronounced at mid-latitudes and in the polar regions. As previously mentioned, in the troposphere a minimum is found in the Northern and Southern Polar Spring. Modulated by this seasonal variability, at all altitudes a constant trend and an inter-hemispherical gradient can also be observed and are further analysed in the subsequent figures. We also notice that for pressures larger than 100 hPa, the CCl_4 measured in the OR phase has a positive bias with respect to that measured in the FR phase. This bias, discussed also in Sect. 4.1, may be due to the different MWs used for the retrieval in the two mission phases, or to the different limb sampling patterns adopted.

Atmos. Chem. Phys. Discuss., doi:10.5194/acp-2016-1163, 2017
Manuscript under review for journal Atmos. Chem. Phys.
Discussion started: 2 March 2017

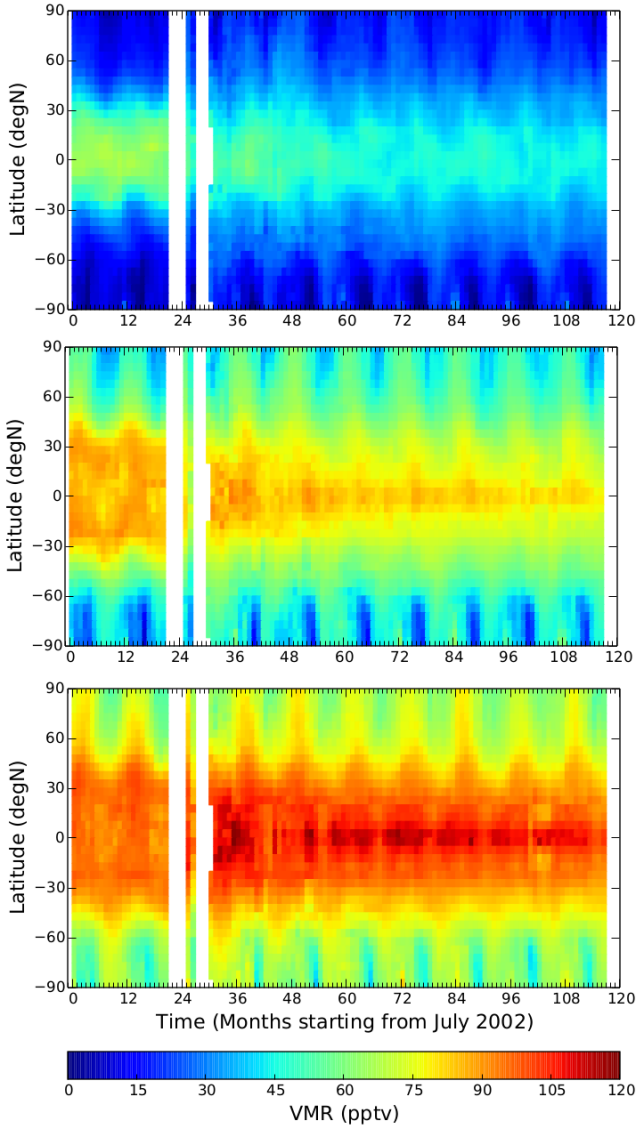

Figure 5. Time evolution of CCl_4 at all latitudes, from July 2002 to April 2012. The three maps refer to different pressure levels: 50 hPa (top), 90 hPa (center) and 130 hPa (bottom).

Figure 6 shows the differences between average CCl_4 profiles measured in the Northern Hemisphere (NH) and in the Southern Hemisphere (SH), as a function of latitude and pressure. The time period employed in the calculated averages extends from April 1^{st}, 2005 to March 31^{st}, 2012. The estimate of the North-South (N-S) differences is important because for long-lived compounds the Inter Hemispheric Gradient (IHG) at the surface is recognized as a qualitative indicator of continuing emissions (Lovelock et al., 1973; Liang et al., 2014). Anthropogenic emissions are larger in the NH, and the transport of these emissions from the NH to the SH takes a year or more. Hence, a significant IHG is evidence of continued emissions driving the

Atmos. Chem. Phys. Discuss., doi:10.5194/acp-2016-1163, 2017
Manuscript under review for journal Atmos. Chem. Phys.
Discussion started: 2 March 2017

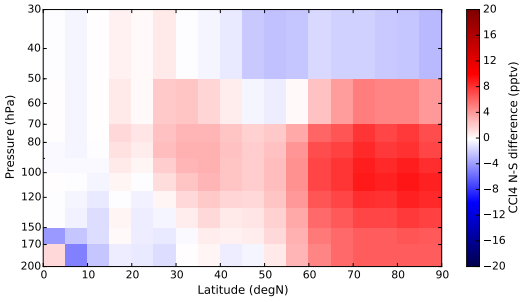

Figure 6. Average North-South CCl_4 VMR differences versus latitude and pressure. The average period includes MIPAS measurements from April 1^{st}, 2005 to March 31^{st}, 2012.

hemispheric differences. At higher altitudes, the asymmetry between the North and South CCl_4 VMR depends not only on the unbalanced emissions at the surface but also on the general circulation of the atmosphere and on seasonal transport. Indeed, we have seen that, especially at high latitudes, N-S differences strongly depend on the season. The large differences visible in Fig. 6 at high latitudes in the stratosphere originate from the subsidence effect during polar winter and spring, bringing mesospheric CCl_4-poor air in the stratosphere. This effect is generally larger in the SH. At mid-latitudes, the CCl_4 VMR differences between NH and SH are less dependent on the season and are mainly due to the larger CCl_4 emissions in the NH.

4 Comparison to other CCl_4 measurements

The most accurate atmospheric CCl_4 measurements are collected at ground level, but such measurements are not suitable for direct comparison with profiles retrieved from MIPAS measurements in the 5-27 km height range. The only CCl_4 profiles suitable for comparison with MIPAS measurements were acquired by the stratospheric balloon version of MIPAS (MIPAS-B, Friedl-Vallon et al. (2004)) and by the ACE-FTS onboard the SciSat-1 satellite (Bernath et al., 2005). In the next two sub-sections we compare MIPAS CCl_4 profiles with co-located profiles obtained from these two instruments.

4.1 Comparison with MIPAS balloon

Stratospheric balloon measurements are particularly suitable for the validation of space-borne limb sounding instruments since these instruments are able to sound the atmosphere with high vertical resolution. The balloon-borne limb emission sounder MIPAS-B can be regarded as a precursor of the MIPAS satellite instrument (Friedl-Vallon et al. (2004) and references therein). Indeed, a number of specifications like spectral resolution ($0.0345\ \mathrm{cm}^{-1}$) and spectral coverage (750–$2500\ \mathrm{cm}^{-1}$) are similar. However, for other parameters the MIPAS-B performance is superior, in particular for the NESR and for the line of sight stabilization, which is based on an inertial navigation system supplemented with an additional star reference system and leads to a knowledge of the tangent altitude on the order of 90 m (3σ). The MIPAS-B NESR is further improved by averaging

Atmos. Chem. Phys. Discuss., doi:10.5194/acp-2016-1163, 2017
Manuscript under review for journal Atmos. Chem. Phys.
Discussion started: 2 March 2017

Atmospheric Chemistry and Physics Discussions

Location	Date	Distance (km)	Time difference (min)
Kiruna (68 N)	20 Mar 2003	16/546	14/15
	03 Jul 2003	Trajectories only	
	11 Mar 2009	187/248	5/6
	24 Jan 2010	109/302	5/6
	31 Mar 2011	Trajectories only	
Aire-sur-l'Adour (44 N)	24 Sep 2002	21/588/410/146	12/13/15/16
Teresina (5 S)	14 Jun 2005	109/497/184/338	228/229/268/269
	06 Jun 2008	224/284/600/194	157/158/169/170

Table 2. Overview of MIPAS balloon flights used for intercomparison with MIPAS/ENVISAT

multiple spectra recorded at the same elevation angle. MIPAS-B limb scans are typically acquired on a 1.5 km vertical tangent height grid.

Retrieval of all species is performed on a 1 km grid with a least squares fitting algorithm using analytical derivative spectra calculated by the Karlsruhe Optimized and Precise Radiative transfer Algorithm (Höpfner et al., 2002; Stiller et al., 2002). To avoid retrieval instabilities due to oversampling of vertical grid points, a regularization approach according to the method described by Tikhonov and Phillips constraining with respect to a first derivative a priori profile is adopted. The spectral window used for the MIPAS-B target parameter retrieval of CCl_4 covers the 786.0–806.0 cm^{-1} interval. Spectroscopic parameters for the calculation of the infrared emission spectra are a combination of the HITRAN 2008 (Rothman et al., 2009) database and the MIPAS dedicated database (Raspollini et al., 2013; Perrin et al., 2016). The CCl_4 cross sections are taken from HITRAN as in MIPAS/ESA retrievals version 7. The MIPAS-B error budget includes random noise as well as covariance effects of the fitted parameters, temperature errors, pointing inaccuracies, errors of non-simultaneously fitted interfering species, and spectroscopic data errors (1σ). For CCl_4 the precision error is estimated to be between 5-10%, while the total error is 11-15%. Further details on the MIPAS-B data analysis and error estimation are provided in Wetzel et al. (2012) and reference therein. Table 2 lists all the MIPAS-B flights used for intercomparison with MIPAS on ENVISAT.

Further than the direct matches where the balloon and the satellite instruments observe simultaneously (within pre-defined margins) the same air-masses, we also considered trajectory matches. In this case both forward and backward trajectories were calculated (Naujokat and Grunow, 2003) by the Free University of Berlin from the balloon measurement geolocation to search for air-masses sounded by the satellite instrument. Temperature and VMR values from the satellite profiles were interpolated to the trajectory match altitude such that these values can be directly compared to the MIPAS-B data at the trajectory start point altitude. To identify both direct and trajectory matches, a coincidence criterion of 1 hour and 500 km was adopted.

Figures 7 and 8 show the average differences between CCl_4 VMR retrieved from MIPAS/ENVISAT and MIPAS-B both in absolute and relative units. The two figures refer to matching measurements in the FR and the OR phases of the MI-

Atmos. Chem. Phys. Discuss., doi:10.5194/acp-2016-1163, 2017
Manuscript under review for journal Atmos. Chem. Phys.
Discussion started: 2 March 2017

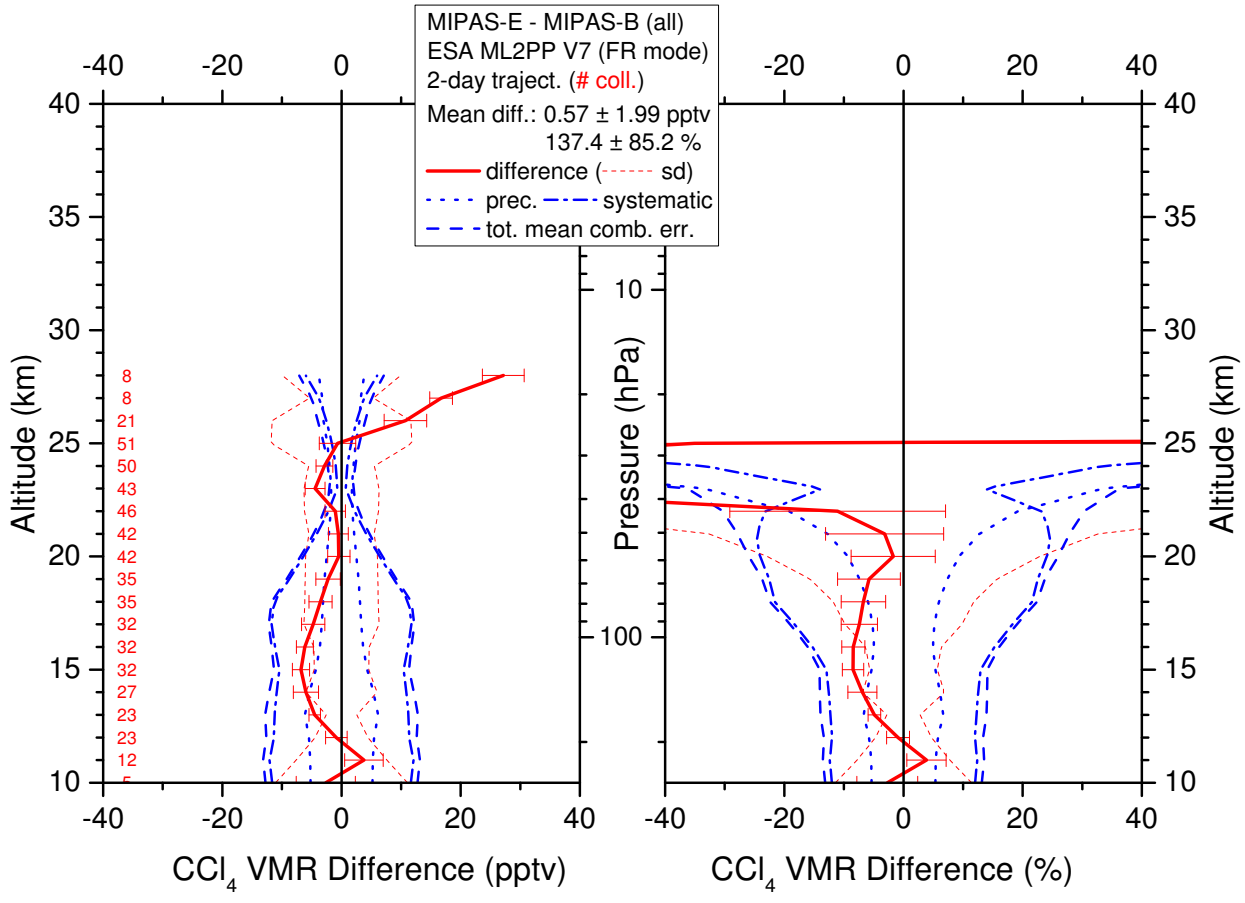

Figure 7. Intercomparison between MIPAS-B and MIPAS/ENVISAT CCl_4 VMR. Results for the FR part of the MIPAS mission.

PAS/ENVISAT mission, respectively. Combined random, systematic and total errors are also shown in the plots. The numbers reported on the left side of the plots indicate the number of matching profiles contributing to the statistics. The results of the intercomparison can be summarized as follows. In the case of FR measurements: for pressures between 80 and 190 hPa MIPAS/ENVISAT shows a statistically significant negative bias of about -10% with respect to MIPAS-B, this bias is however within the combined total error bounds. A statistically significant positive bias is also evident for pressures smaller than 25 hPa. It increases with altitude and quickly becomes incompatible with the total combined error. This bias, however, is not a major concern because it is localized at the upper end of the retrieval range. In this region the predicted uncertainty is so large that the linear approximation of the error propagation theory may easily fail to explain the discrepancies between the measurements of the two instruments. In case of OR measurements: for pressures between 150 and 190 hPa MIPAS/ENVISAT shows a statistically significant positive bias of about $+10\%$ with respect to MIPAS-B; this bias is however within the combined total error bounds. A statistically significant positive bias is also evident for pressures smaller than 25 hPa. It increases with altitude

Atmos. Chem. Phys. Discuss., doi:10.5194/acp-2016-1163, 2017
Manuscript under review for journal Atmos. Chem. Phys.
Discussion started: 2 March 2017

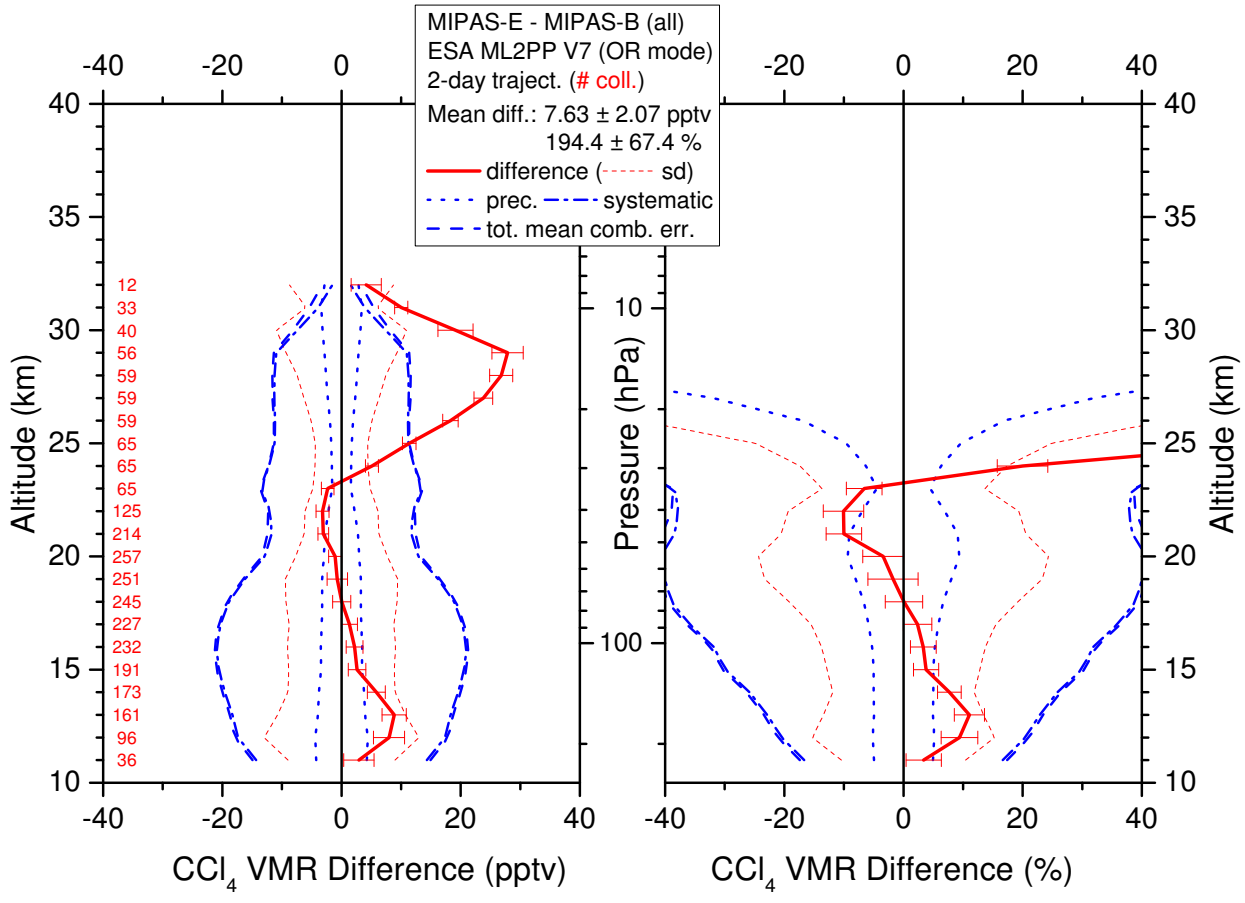

Figure 8. Intercomparison between MIPAS-B and MIPAS/ENVISAT CCl_4 VMR. Results for the OR part of the MIPAS mission.

and, for pressures smaller than 20 hPa is no longer compatible with the total combined error. As in the FR case, this large bias occurs at the upper end of the MIPAS/ENVISAT retrieval range where the predicted combined error is very large. Furthermore, validation with ACE (see next Section) indicates a negative bias of MIPAS wrt ACE-FTS, in the same altitude region, hence MIPAS/ENVISAT is in the middle between MIPAS balloon and ACE-FTS.

4.2 Comparison with ACE-FTS V3.5

ACE-FTS is a Canadian solar occultation limb sounder operating since 2004 from SciSat in a low (≈ 650 km) circular orbit. The measured spectra cover the region from 750 to 4400 cm^{-1} with a spectral resolution of 0.02 cm^{-1} (Bernath et al., 2005). Several target atmospheric parameters are routinely retrieved from ACE-FTS measurements. Among them, temperature, pressure, and the VMR profiles of over 30 atmospheric trace gases and over 20 subsidiary isotopologues. Profiles are retrieved in the range from $\sim$ 5 to 150 km, with a vertical field of view of $\sim$ 3-4 km and a vertical sampling of 2-6 km. The ACE-FTS retrieval

Atmos. Chem. Phys. Discuss., doi:10.5194/acp-2016-1163, 2017
Manuscript under review for journal Atmos. Chem. Phys.
Discussion started: 2 March 2017

Atmospheric Chemistry and Physics Discussions

algorithm is described in Boone et al. (2005), and the updates for the most recent version of the retrieval, version 3.5, are detailed in Boone et al. (2013). The retrieval algorithm uses a non-linear least-squares global-fitting technique that fits the ACE-FTS observed spectra in given microwindows with forward modelled spectra based on line strengths and line widths from the HITRAN 2004 database (Rothman et al., 2005) (with updates as described by Boone et al. (2013)). Pressure and temperature profiles used in the forward model are the ACE-FTS derived profiles, calculated by fitting CO_2 lines. The spectral window used for CCl_4 retrievals goes from 787.5 to 805.5 cm^{-1}.

Several hundred ACE-FTS measurements are coincident with MIPAS soundings of the OR part of the mission. These measurements are located both in the Northern and Southern hemispheres, mainly at latitudes larger than 45°. For comparison with MIPAS, all ACE-FTS CCl_4 data used were screened using the v3.5 quality flags. As recommended by Sheese et al. (2015), any profile data point with flag value of 2 or greater was removed and any profile containing a flag value between 4 and 7, inclusive, was discarded. For intercomparison with MIPAS measurements we adopted a matching criterion of 3 hours and 300 km. We also tested different matching criteria, such as 2 hours and 300 km, 3 hours and 200 km, but found no significant changes in the validation results. First we interpolated the matching MIPAS and ACE-FTS CCl_4 profiles to a fixed set of pressure levels. Then we grouped the profile differences in latitudinal intervals. The results of the comparison are summarized in Fig. 9. Each of the four plots of the figure refers to one of the considered latitude intervals: 50–70° and 70–90° in both the Southern and the Northern hemispheres. Each plot shows the average CCl_4 difference profile between co-located MIPAS and ACE-FTS measurements (red) with standard deviation of the mean (red error bars). The standard deviation of the difference (orange), the total random error (green), the total systematic error of the difference (blue) are also shown. The number of co-located pairs contributing at each pressure level is reported on the right side of each plot. The average difference (red line) quantifies the systematic bias between ACE-FTS and MIPAS, the error bars indicate its statistical significance. The standard deviation (orange) is an *ex-post* estimate of the combined random error of the individual profile differences and, therefore, should be similar to its *ex-ante* estimate represented in the plots by the green line. We calculated the ex-ante random error of the individual profile differences as the quadrature summation of the ACE-FTS and MIPAS random errors. The ACE-FTS random error is estimated via the noise error covariance matrix of the retrieval included in the Level 2 products. The MIPAS random error is estimated as the quadrature summation of the measurement noise error evaluated by the covariance matrix of the retrieval (Ceccherini and Ridolfi, 2010) and the other error components that are expected to change randomly in our sample, i.e. the errors that we classified of types a) and b) in Sect. 2.1. The systematic error of the profile differences is obtained as the quadrature summation of the ACE-FTS and the MIPAS errors that are constant within the sample and are not expected to bias in the same direction the measurements of the two instruments. On the basis of the error figures suggested by Allen et al. (2009), for ACE-FTS we assumed a 20% systematic error constant at all pressure levels. For MIPAS we calculated the quadrature summation of systematic errors that in Sect. 2.1 we classified as of type c) and d). For the calculation of the combined systematic error we explicitly excluded the uncertainty in the CCl_4 cross-section data (Rothman et al., 2005) that are used, approximately in the same spectral region, both in MIPAS and ACE-FTS retrievals.

Apart from the latitude interval from 50 to 70° S, the systematic differences between MIPAS and ACE-FTS are within 5 pptv (~ 10 %, mostly not significant from the statistical point of view) in the pressure range from 50 to 100–110 hPa.

Atmos. Chem. Phys. Discuss., doi:10.5194/acp-2016-1163, 2017
Manuscript under review for journal Atmos. Chem. Phys.
Discussion started: 2 March 2017

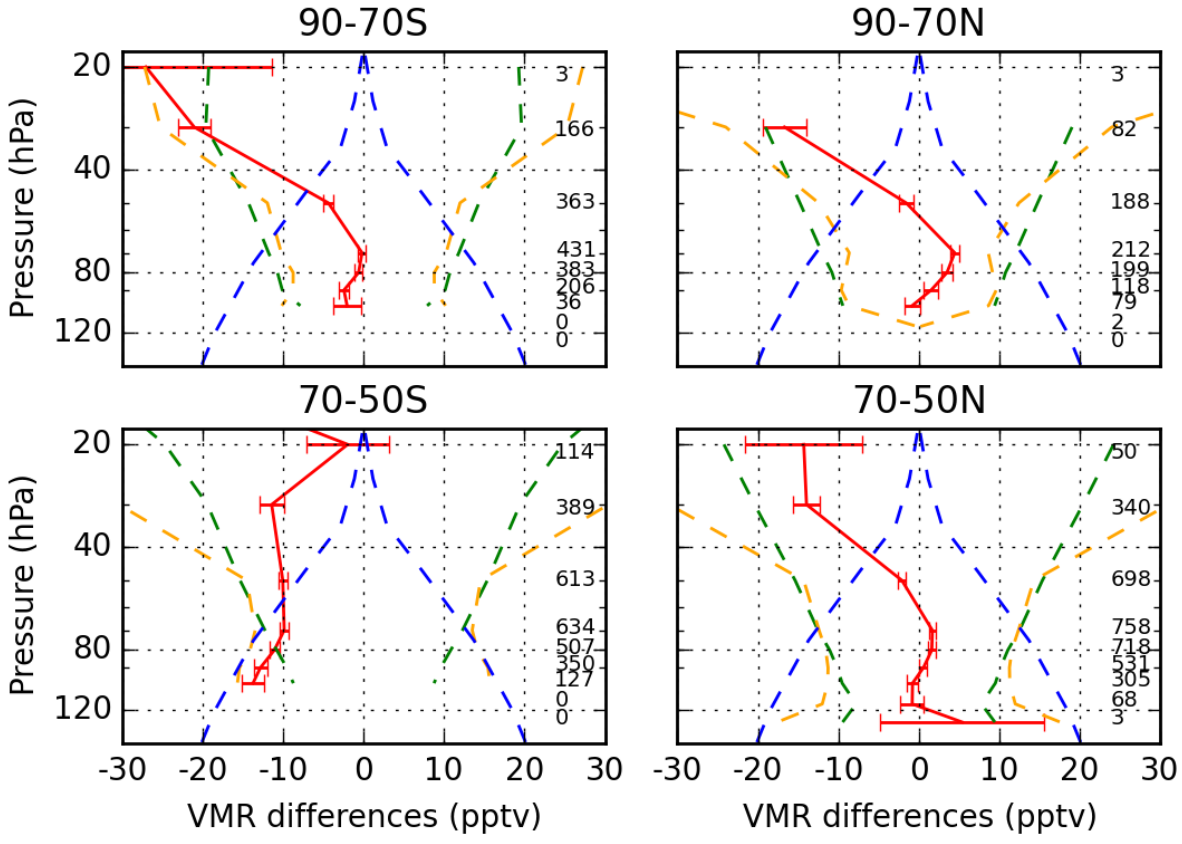

Figure 9. Mean CCl_4 profile difference between co-located MIPAS and ACE-FTS measurements (red) with standard deviation of the mean (red error bars). The standard deviation of the differences (orange), the estimated total random (green) and total systematic (blue) errors of the difference are also shown The number of co-located pairs for each pressure level is reported on the right side of each graph. Each plot refers to a latitude interval as indicated in the title.

The amplitude of systematic differences increases up to 15–20 pptv and becomes statistically significant at 30 hPa, while it is again quite small at 20 hPa. In the latitude interval from 50 to 70° S we observe a statistically significant ≈ 10 pptv low bias of MIPAS with respect to ACE-FTS, almost uniform over the entire retrieval height range. At all latitudes, the observed biases are compatible with the estimated combined systematic error only for pressures greater than 40 hPa. At 30 hPa the bias is statistically significant and incompatible with error bars. The reason for this inconsistency is still unclear; however, preliminary investigations show that the inconsistency will be reduced when using the future release version 4.0 of ACE-FTS products.

The ex-ante estimate of the combined random error (green line in Fig. 9) agrees pretty well with the ex-post estimated standard deviation of the profile differences (orange line) in the range between 40 and 80–100 hPa. At the edges of the retrieval range the observed variability of the differences generally exceeds the ex-ante estimate of the random error. This may be due

Atmos. Chem. Phys. Discuss., doi:10.5194/acp-2016-1163, 2017
Manuscript under review for journal Atmos. Chem. Phys.
Discussion started: 2 March 2017

Atmospheric Chemistry and Physics Discussions

both to the fact that our ex-ante random error estimate does not take into account the imperfect matching of the compared profiles, and to the fact that, at these specific altitudes, the sensitivity of the measurements to the CCl_4 VMR is so low that the linear approximation of the error propagation theory could provide only rough error estimates.

As a final remark we note that at 30 hPa MIPAS-B (Fig. 8) and ACE-FTS (Fig. 9) intercomparisons provide contrasting indications on the MIPAS bias in the OR part of the mission. While MIPAS-B suggests a positive MIPAS bias of about 10 pptv, ACE-FTS points to a negative bias of $10-20$ pptv.

5 Trends

5.1 Trend calculation method

The measurements used for the analysis presented in this study cover the entire MIPAS mission, from July 2002 to April 2012. The CCl_4 VMR profiles considered are those derived by the ESA Level 2 processor version 7 analysing MIPAS limb scanning measurements with tangent heights in the 6-70 km range, obtained from nominal (NOM), middle atmosphere (MA) and Upper Troposphere Lower Stratosphere (UTLS1) observational modes (Raspollini et al., 2013).

First we linearly interpolate in log-pressure all the considered CCl_4 VMR profiles to the 28 SPARC (Stratospheric Processes and their Role in Climate) data initiative (Hegglin and Tegtmeier, 2011) pressure levels (300, 250, 200, 170, 150, 130, 115, 100, 90, 80, 70, 50, 30, 20, 15, 10, 7, 5, 3, 2, 1.5, 1.0, 0.7, 0.5, 0.3, 0.2, 0.15, 0.1 hPa). We then group the interpolated profiles in 5° latitude bins and calculate monthly averages. Finally, using the least-squares method, for each latitude bin and pressure level we fit the following function $\mathrm{VMR}(t)$ to the time series of the monthly averages:

$$\begin{aligned}\mathrm{VMR}(t) = {} & a_{\mathrm{FR}}\,\mathbf{1}_{\mathrm{FR}}(t) + a_{\mathrm{OR}}\,\mathbf{1}_{\mathrm{OR}}(t) + bt + f_1\,\mathrm{qbo30}(t) + f_2\,\mathrm{qbo50}(t) + \\ & + g\,\mathrm{SRF}(t) + \sum_i \left[c_i \sin\left(\frac{2\pi t}{T_i}\right) + d_i \cos\left(\frac{2\pi t}{T_i}\right)\right].\end{aligned} \tag{1}$$

In this expression t is the time expressed in months since the beginning of the mission (July 2002) and a_{FR}, a_{OR}, b, f_1, f_2, g and c_i, d_i, $i = 1, ..., 8$ are the 22 fitting parameters. The function $\mathbf{1}_{\mathrm{P}}(t)$ is the indicator function of the time interval P, such that $\mathbf{1}_{\mathrm{P}}(t) = 1$ if $t \in \mathrm{P}$ and $\mathbf{1}_{\mathrm{P}}(t) = 0$ otherwise. The functions $\mathrm{qbo30}(t)$ and $\mathrm{qbo50}(t)$ are the quasi-biennial oscillation (QBO) quantifiers and $\mathrm{SRF}(t)$ is the solar radio flux index. The two QBO terms (available at http://www.geo.fu-berlin.de/met/ag/strat/produkte/qbo/index.html) represent the Singapore winds at 30 and 50 hPa (Kyrölä et al., 2010). The SRF index is calculated using measurements of the solar flux at 10.7 cm (available at http://lasp.colorado.edu/lisird/tss/noaa_radio_flux.html) and is considered a good proxy for the solar activity. We re-normalized both the QBO and the SRF proxies to the interval $[-1, +1]$ within the time frame covered by MIPAS mission. The terms in the sum are 8 sine and 8 cosine functions. They represent periodic oscillations with period T_i. In T_i we include annual (12 months), semi-annual (6 months) and other characteristic atmospheric periodicities of 3, 4, 8, 9, 18 and 24 months. We decided to fit two different offset parameters for the two parts of the mission: a_{FR} for the FR and a_{OR} for the OR part. The aim of this choice is to account for possible relative biases

Atmos. Chem. Phys. Discuss., doi:10.5194/acp-2016-1163, 2017
Manuscript under review for journal Atmos. Chem. Phys.
Discussion started: 2 March 2017

Atmospheric Chemistry and Physics Discussions

between the two phases of the mission. These may be caused, for example, by the different spectral resolutions adopted, by the different MWs used for the retrieval and by the different vertical and horizontal samplings of the instrument in the two mission phases. We calculate the uncertainty on the fitted parameters assuming each monthly average is affected by an error given by the standard deviation of the mean. Furthermore we multiply the uncertainty obtained from the error propagation analysis by the square root of the normalized least squares (the so-called "reduced χ^2"). This latter operation is intended to account also for the quality of the fit in the evaluation of trend errors.

5.2 Results

Figure 10 shows some examples of CCl_4 trend analysis. Each panel refers to a specific latitude band and pressure level. The top plot of each panel shows the time series of the monthly averages with error bars given by the standard deviation of the mean (blue symbols). The red curve represents the best fitting function $\mathrm{VMR}(t)$, while the green line represents the constant and the linear (trend) terms of $\mathrm{VMR}(t)$. In the lower plot of each panel we show the residuals of the fit (the monthly averages minus the values calculated on the fitting curve). In each panel we also report the value obtained for the trend, its uncertainty and the difference between the two offset terms $a_{FR} - a_{OR}$.

The quality of the fit is generally better in the OR period. Indeed, in this mission phase the instrument provides measurements with more uniform and finer geographical coverage. We also carried-out a careful spectral analysis of the residuals of the fits. Although not reported here for reasons of brevity, this analysis reveals that all the periodicities embedded in the considered time series of monthly means are properly accounted for by the fitting function (1).

Figure 11 summarizes the results obtained for CCl_4 trends. Panel a) shows the absolute trends. Negative trends are observed at all latitudes in the UTLS region. The magnitude of the negative trend decreases with increasing altitude. The trend shows slightly positive values (about 5-10 pptv/decade) in a limited region, particularly in the Southern mid-latitudes between 50 and 10 hPa. This feature is probably related to the asymmetry in the general circulation of the atmosphere. The air at higher altitudes can be considered *older* than the tropospheric air that has been lifted up by strong convection mechanisms in the tropical regions (Stiller et al., 2012). The tropospheric air just injected into the stratosphere is richer in CCl_4. We attribute positive stratospheric trend values in certain latitude regions to the less effective mixing mechanisms in the stratosphere as compared to the troposphere at these latitudes. Similar features have also been observed by other authors in CFC-11 and CFC-12 trends (Kellmann et al., 2012).

Assuming for each latitude bin and pressure level the average CCl_4 VMR obtained from the full MIPAS dataset, we also calculated the relative CCl_4 trends. They are shown in the panel b) of Fig. 11. The same considerations made for the absolute trends apply also to relative trends. The asymmetry between the NH and the SH is very pronounced, the NH having larger negative relative trends increasing with altitude and reaching 30-35%/decade at 50 hPa. Note however that above 50 hPa they show large variations with both latitude and pressure. These oscillations correspond to extremely small average VMR values that make the relative trend numerically unstable. Panels c) and d) of Fig. 11 show, respectively, the absolute and percentage random errors on the trends. The uncertainties increase above 20 hPa. Large uncertainties are associated to latitude bins and pressure levels for which a relatively small number of measurements is available. For clarity in Fig. 12 we show the ratio

Atmos. Chem. Phys. Discuss., doi:10.5194/acp-2016-1163, 2017
Manuscript under review for journal Atmos. Chem. Phys.
Discussion started: 2 March 2017

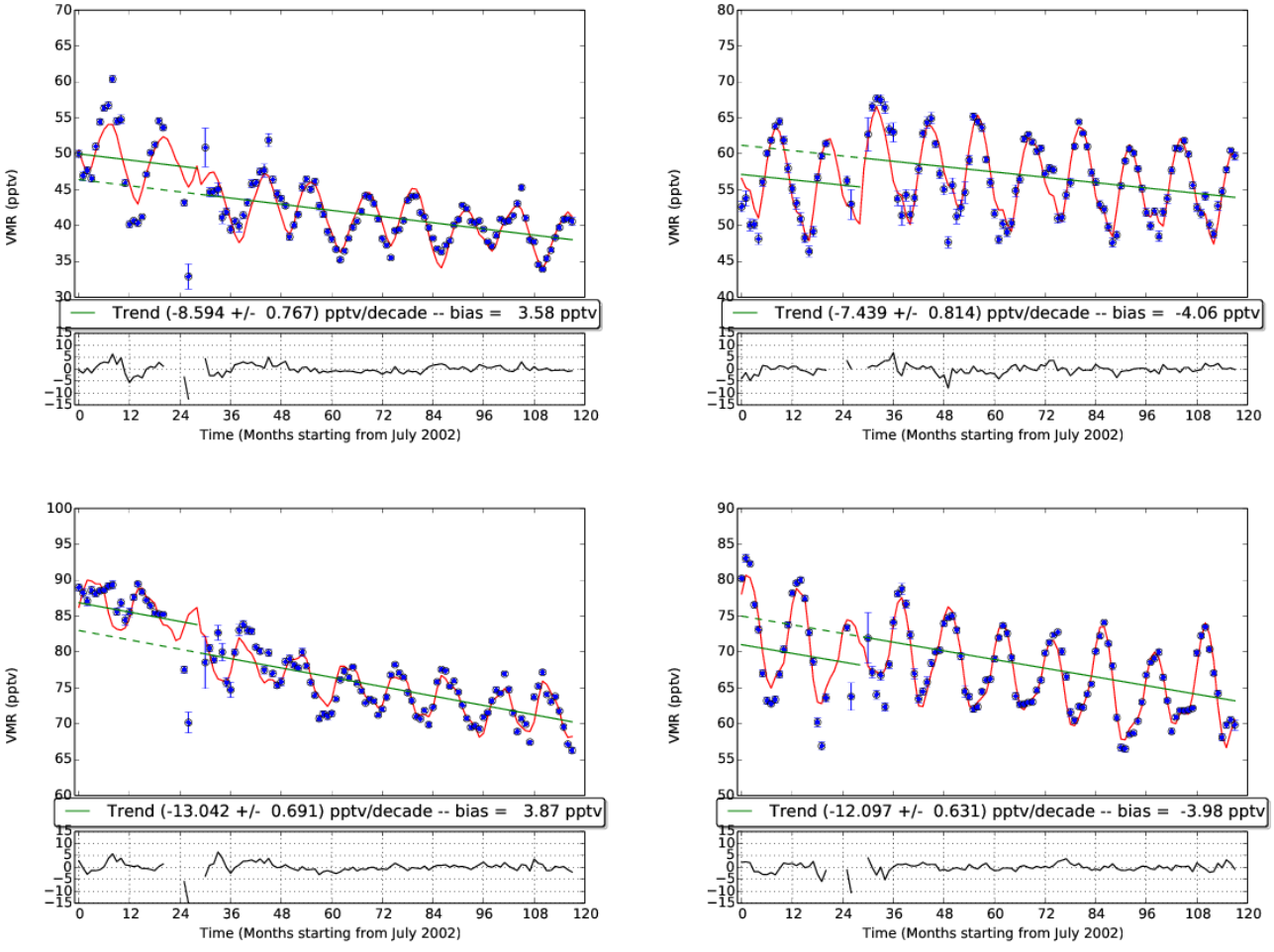

Figure 10. CCl_4 trend analysis for 20° S/25° S at 50 hPa (top left), 55° S/60° S at 100 hPa (top right), 25° N/20° N at 90 hPa (bottom left) and 50° N/45° N at 100 hPa (bottom right). The blue dots are the MIPAS monthly averages and the error bars are the standard deviation of the means. The red curve is the best fitting function $\mathrm{VMR}(t)$ and green line is the linear term (trend). The lower part of each plot shows the residuals between the MIPAS monthly averages and the best fitting function $\mathrm{VMR}(t)$. The CCl_4 trend, its uncertainty and the *bias* between FR and OR are also indicated in each panel.

between CCl_4 trends and the related random errors. Latitude bins / pressure levels with ratio values less than 2 are marked with white and grey colors and correspond to trend values that are not significantly different from zero from the statistical point of view. Note, however, that most of the calculated trends are greater than 5 times the related error, and are thus statistically significant. In the maps of Fig.s 11 and 12, values corresponding to errors greater than 30% are masked with dashes. We consider unreliable any trends reported here with errors greater than this threshold.

Atmos. Chem. Phys. Discuss., doi:10.5194/acp-2016-1163, 2017
Manuscript under review for journal Atmos. Chem. Phys.
Discussion started: 2 March 2017

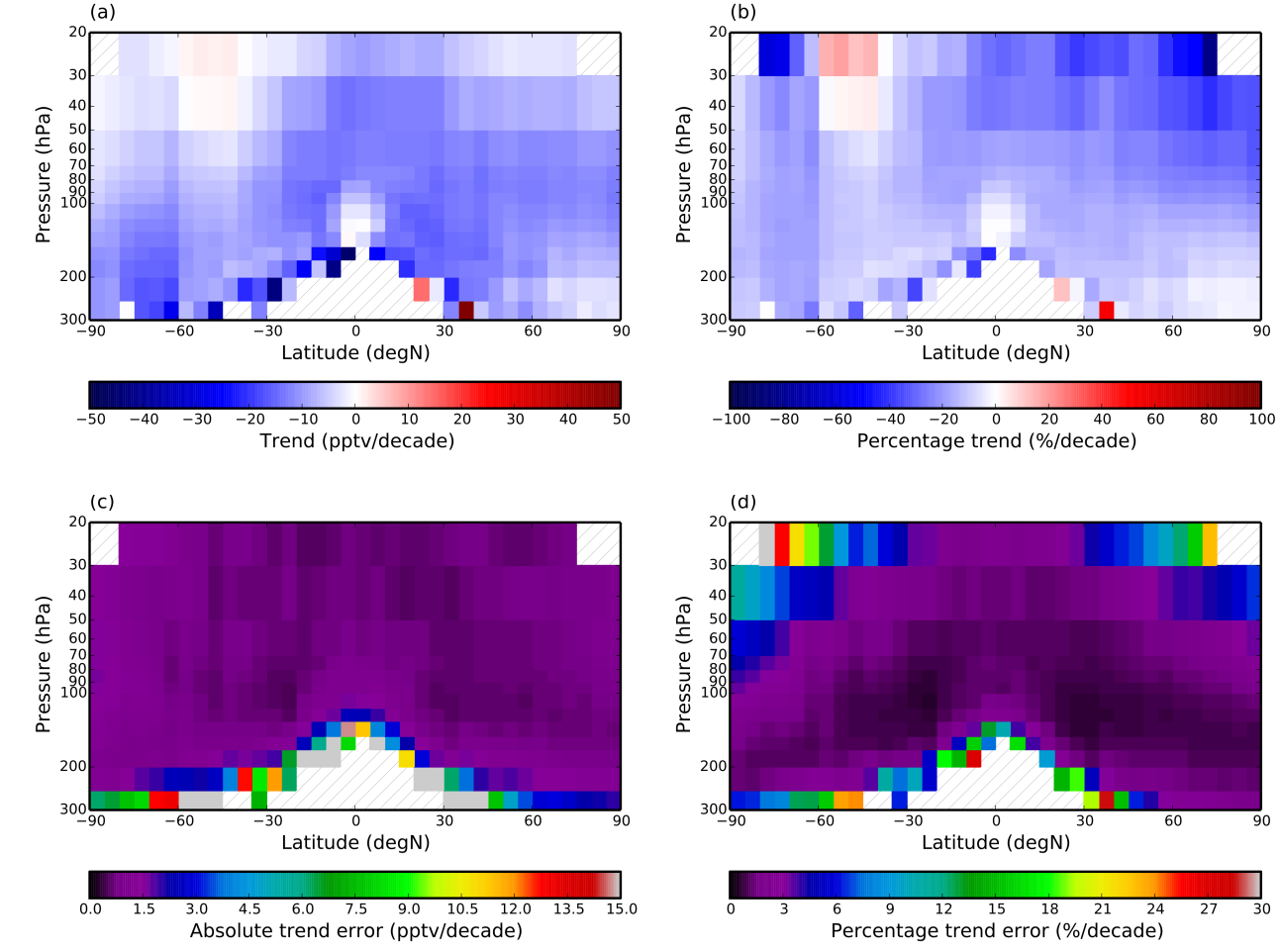

Figure 11. CCl_4 trends as a function of latitude and pressure. Panel a) absolute trends, b) percentage trends, c) absolute errors, d) percentage errors. Latitudes / pressures with trend error greater than 30% are masked with dashed areas.

As mentioned in Sect. 2.1, an important source of uncertainty could arise from a residual drift of the calibration error, possibly due to neglecting changes in detector non-linearity as the instrument ages. As outlined in Sect. 2.1, however, the worst case scenario for the drift of the calibration error could amount to 1% of the calibration error itself, which in turn, is of the order of 0.4% of each individual retrieved CCl_4 VMR profile. Therefore, this error source is negligible compared to the statistical error shown in the right panel of Fig. 11.

Atmos. Chem. Phys. Discuss., doi:10.5194/acp-2016-1163, 2017
Manuscript under review for journal Atmos. Chem. Phys.
Discussion started: 2 March 2017

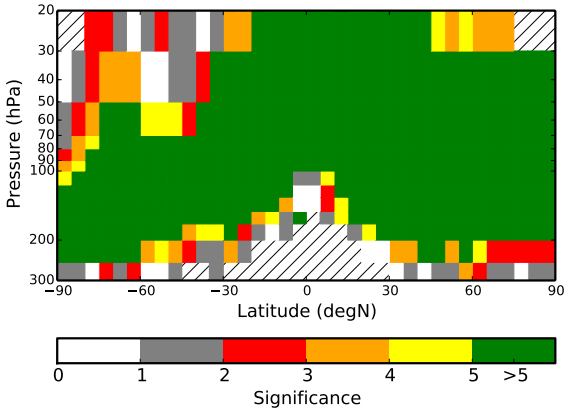

Figure 12. Map of the ratio between CCl_4 trends and associated random errors.

5.3 Comparison with CCl_4 trends reported in literature

Although measurements acquired at ground stations cannot be directly compared with MIPAS profiles that have a lower altitude limit of 5-6 km, we can still compare tropospheric CCl_4 trends derived from MIPAS with trends derived from ground-based measurements. In particular, we consider observations provided by two networks that regularly perform long-term, highly accurate near-surface measurements of various tracers, including CCl_4: the NOAA/ESRL/HATS (http://www.esrl.noaa.gov/gmd/hats/) and the AGAGE (Simmonds et al., 1998; Prinn et al., 2000, 2016) http://agage.mit.edu/) networks. The NOAA/ESRL/HATS group provides accurate measurements of CCl_4 through three different programs: two in situ electron capture detector (ECD) measurement programs and one flask system using gas chromatography with ECD program. In this work we use a CCl_4 combined dataset, developed by the NOAA to homogenize all of the measurements made by the different programs (more details at http://www.esrl.noaa.gov/gmd/hats/combined/CCl4.html). All the CCl_4 NOAA records are reported on the NOAA-2008 scale. AGAGE measurements used here are obtained using in situ gas chromatography with ECD and reported on the SIO-2005 calibration scale. NOAA and AGAGE in situ measurements at common sites are inter-compared every 6 months for validation purposes.

To compare MIPAS CCl_4 trends to those derived from the ground-based measurements of NOAA and AGAGE, we first choose a pressure level belonging to the troposphere, with the following procedure. For each latitude bin (λ) and MIPAS monthly average profile we identify the tropopause with the pressure level where the monthly average temperature shows its minimum value. We multiply this pressure by 1.6 and find the nearest pressure level ($p_t(\lambda)$) in the fixed pressure grid defined in Sect. 5.1. For each latitude bin and month we then compute the monthly CCl_4 average at $p_t(\lambda)$. Finally, for each latitude bin, we calculate the trend at this month- and latitude- dependent tropospheric pressure as explained in Sect. 5.1.

Atmos. Chem. Phys. Discuss., doi:10.5194/acp-2016-1163, 2017
Manuscript under review for journal Atmos. Chem. Phys.
Discussion started: 2 March 2017

Atmospheric Chemistry and Physics Discussions

Figure 13 compares the time series of ground-based CCl_4 measurements of selected stations (black and orange lines) with MIPAS monthly tropospheric averages (blue dots) in the same latitude bin of the ground station. The two plots refer to ground stations located at tropical (top) and middle (bottom) latitudes. Ground-based measurements do not really show a seasonality, while MIPAS measurements do. The amplitude of the seasonal variations observed by MIPAS increases with latitude. For tropical latitudes MIPAS OR measurements show a positive bias of approximately 15%. Although not focused on tropical regions, Fig. 8 comparing MIPAS to balloon measurements, already suggests the existence of this bias. At middle latitudes the maximal values of the MIPAS time series roughly match ground measurements. In Fig. 13 we also show the trend values determined on the basis of the plotted measurements. In the examined cases the trends obtained from MIPAS and ground stations are in very good agreement.

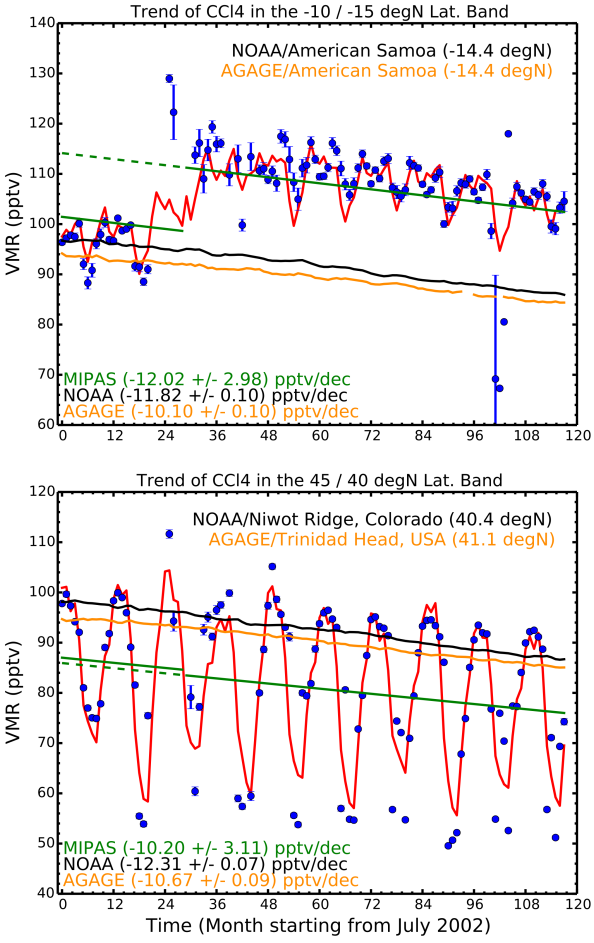

Figure 13. Comparison between MIPAS (blue dots) and NOAA/AGAGE (black/orange) CCl_4 time series. The two plots refer to ground stations located at tropical (top) and middle (bottom) latitudes. The red curve is the fitting model used to derive the trend from MIPAS data, the green line is the linear part of the model itself. The obtained trend values are also shown in the plots.

Atmos. Chem. Phys. Discuss., doi:10.5194/acp-2016-1163, 2017
Manuscript under review for journal Atmos. Chem. Phys.
Discussion started: 2 March 2017

Atmospheric Chemistry and Physics Discussions

Site Code	Site Name	Latitude (degN)	Network	In-situ trend (pptv/decade)	MIPAS trend (pptv/decade)	MIPAS Lat. Band (degN)
BRW	Barrow, USA	71.3	NOAA	-12.7	-3.2 ± 10.4	70/75
MHD	Mace Head, Ireland	53.3	AGAGE	-10.1	-4.7 ± 5.1	50/55
THD	Trinidad Head, USA	41.1	AGAGE	-10.6	-10.2 ± 3.1	40/45
NWR	Niwot Ridge, USA	40.4	NOAA	-12.3	-10.2 ± 3.1	40/45
MLO	Mauna Loa, USA	19.5	NOAA	-12.2	-14.9 ± 2.3	15/20
RPB	Ragged Point, Barbados	13.2	AGAGE	-10.7	-12.7 ± 3.6	10/15
SMO	Tatuila, American Samoa	-14.4	NOAA AGAGE	-11.8 -10.1	-12.0 ± 3.0	$-10/-15$
CGO	Cape Grim, Tasmania	-40.7	AGAGE	-10.2	-25.9 ± 5.4	$-40/-45$
SPO	South Pole, Antartica	-90.0	NOAA	-11.9	-7.9 ± 10.6	$-85/-90$

Table 3. For each ground station the table columns show respectively: site code, site name, site latitude, network name, station-related CCl_4 trend, tropospheric MIPAS trend, latitudinal band from which MIPAS data were extracted.

In Table 3 we compare MIPAS tropospheric CCl_4 trends with trends derived for the 2002–2012 decade from NOAA/AGAGE stations located in the same latitude band. As we can see, some stations produce CCl_4 trends in very good agreement with MIPAS. However, in general, and especially in the polar regions, the variability of the tropopause is quite large, thus producing time series of MIPAS monthly averages at $p_t(\lambda)$ that can not be adequately matched by the fitting function defined in Eq. 1. This feature sometimes generates large residuals in the trend fit and thus large trend errors and/or unrealistic trend values. Despite this difficulty, from the statistical point of view the only trends calculated at the CGO site disagree significantly. We attribute this disagreement to the instabilities occurring in MIPAS data at low altitudes. Indeed, the MIPAS tropospheric trend estimated for the latitude bin $35°/40°$ S (the bin adjacent to the CGO site) is already equal to -9.16 ± 2.03 pptv/decade, i.e. in perfect agreement with the trend calculated from the CGO measurements.

Looking at the literature we found that Brown et al. (2011) estimate a kind of global CCl_4 trend from ACE-FTS measurements. The authors consider CCl_4 VMR profiles obtained from ACE-FTS in the 30° S/30° N latitude belt. They calculate

Atmos. Chem. Phys. Discuss., doi:10.5194/acp-2016-1163, 2017
Manuscript under review for journal Atmos. Chem. Phys.
Discussion started: 2 March 2017

Atmospheric Chemistry and Physics Discussions

yearly averages of CCl_4 VMR in the altitude range from 5 to 17 km and fit the seven 2004-2010 yearly averages with a linear least-squares approach. The resulting trend is -13.2 ± 0.9 pptv/decade. If we average MIPAS trends presented in Sect. 5.2 in the 30° S/30° N latitude interval and in the 100–300 hPa pressure range, with a filter discarding trend values with relative error greater than 30%, we get an average trend of -12.80 ± 0.12 pptv/decade. This value is in very good agreement with the trend determined from ACE-FTS. Note also that, since MIPAS measures atmospheric emission its sampling is finer than that of ACE-FTS both in space and time. With MIPAS it is therefore possible to achieve a smaller trend error.

6 Lifetime

In this Section we estimate the stratospheric lifetime of CCl_4 using tracer-tracer linear correlations in the lower stratosphere, as described in Plumb and Ko (1992). The lifetime can be calculated using the following equation:

$$\frac{\tau_1}{\tau_2} = \frac{d\sigma_2}{d\sigma_1} \cdot \frac{\sigma_1}{\sigma_2} \tag{2}$$

where τ_1 and τ_2 are the stratospheric lifetimes of the two selected tracers, $d\sigma_2/d\sigma_1$ is the slope of the correlation and σ_1, σ_2 are the tropospheric VMRs of the two species. The tracers with known lifetime employed in this study are CFC-11 and CFC-12. As suggested in Brown et al. (2013), for this study we consider only the latitudes in the so-called *surf* zone (Volk et al., 1997), between 30° N/S and 70° N/S. The tropical regions are not suitable to estimate the stratospheric lifetime using the tracer-tracer method due to the intense large-scale upwelling (Plumb and Ko, 1992). Similarly, the polar regions are not suitable for this study due to the intense subsidence, especially during winter (Plumb, 2007). For each month of the MIPAS mission and each 5° latitudinal band between 30° N/S and 70° N/S, we determine the pressure level corresponding to the tropopause, taken as the level with a minimum in the monthly average temperature profile. For each latitudinal band, we determine the slope of the correlation considering only the VMR monthly averages of CFC-11 (or CFC-12) and CCl_4 at the subset of SPARC pressure levels (see Sect. 5.1) above the tropopause. As suggested in Brown et al. (2013), we apply additional filters to the VMRs of CFC-11 and CFC-12. We consider only VMRs greater than 100 pptv for CFC-11 and greater than 300 pptv for CFC-12. This approach makes us confident that the calculated slope is not affected by VMR values associated with the upper stratosphere. We compute the tropospheric VMR values of the three species by averaging the MIPAS retrieved VMR values at the SPARC pressure level below the tropopause. For CFC-11 we assume a lifetime of 52(43 - 67) years and for CFC-12 a lifetime of 102(88 - 122) years, as recommended in SPARC (2013). The results of our analysis are reported in Table 4. The global average lifetime turns out to be 46(38 - 60) years considering CFC-11 as the correlated tracer, and 48(41 - 58) years considering CFC-12. These estimates are consistent with the most recent literature that suggests an atmospheric lifetime of 44(36 - 58) years (SPARC, 2013, 2016). Several older studies report atmospheric CCl_4 lifetimes between 30 and 50 years (Singh et al., 1976; Simmonds et al., 1988; Montzka et al., 1999; World Meteorological Organization (WMO), 1999; Allen et al., 2009). In Brown et al. (2013) the authors study the stratospheric lifetime of several species (including CFC-11, CFC-12 and CCl_4) using ACE-FTS measurements. Using a CFC-11 lifetime of 45±7 (World Meteorological Organization (WMO),

Atmos. Chem. Phys. Discuss., doi:10.5194/acp-2016-1163, 2017
Manuscript under review for journal Atmos. Chem. Phys.
Discussion started: 2 March 2017

Atmospheric Chemistry and Physics Discussions

	Global Average Lifetime (years)	NH Average Lifetime (years)	SH Average Lifetime (years)
CFC-11	$46(38-60)$	$47(39-61)$	$45(38-59)$
CFC-12	$48(42-58)$	$47(41-56)$	$49(42-59)$

Table 4. CCl_4 lifetime calculated using the tracer-tracer linear correlations with CFC-11 and CFC-12 in the lower stratosphere for the entire globe, the Northern and the Southern hemispheres.

2011) these authors calculate a CCl_4 global lifetime of 35±11 years. The difference with our results is explained taking into account the different reference CFC-11 lifetimes used: using the same CFC-11 lifetime (World Meteorological Organization (WMO), 2011) we would obtain a CCl_4 lifetime of 40±7 years. As in Brown et al. (2013) we also computed the CCl_4 lifetime separately in the two hemispheres, identifying consistent values: 47(39 - 61) years in the NH and 45(38 - 59) years in the SH. By contrast, Brown et al. (2013) report very different lifetimes in the two hemispheres (41±9 years in the NH and 21±6 years in the SH) but they are not able to provide a solid justification for this finding. Again, the differences with our results are partially explained with the different CFC-11 lifetime considered (using the same CFC-11 lifetime (World Meteorological Organization (WMO), 2011) we would obtain a CCl_4 lifetime of 41±8 years in the NH and 39±6 years in the SH) but the choice of different reference lifetimes does not explain the hemispheric asymmetry reported in Brown et al. (2013). We also calculated CCl_4 lifetimes in the two hemispheres considering CFC-12 as correlated tracer and we obtained a lifetime of 47(41 - 57) years in the NH and of 49(42 - 59) years in the SH.

7 Conclusions

The ESA Version 7 processor has been used to retrieve for the first time the CCl_4 VMR global distribution in the UTLS using MIPAS measurements. The CCl_4 MIPAS observations cover the altitude range from 6 to 27 km and, having been obtained from emission measurements, provide a global coverage. The zonal means of CCl_4 VMR show features typical of long-lived species of anthropogenic origin that are destroyed primarily in the stratosphere by photolysis. The highest VMR values are found in the troposphere, and VMR monotonically decreases with increasing altitude in the stratosphere. In the lower stratosphere, the largest values are observed between 30°S and 30°N due to the intense updraft that occurs in the tropical region. The CCl_4 global distribution shows also a seasonal variability. This seasonality is more evident in the polar regions due to CCl_4-poor mesospheric air subsidence induced by the polar vortex.

We calculated the IHG in the UTLS using average CCl_4 profiles measured in the NH and in the SH. At high latitudes in the stratosphere, differences the order of 10-15 pptv are observed, showing a strong seasonal variation, caused by subsidence (generally more intense in the SH) during polar winter and spring. At mid-latitudes, the CCl_4 VMR differences between the two hemispheres are less dependent on the season and are mainly caused by the larger CCl_4 emissions in the NH.

Atmos. Chem. Phys. Discuss., doi:10.5194/acp-2016-1163, 2017
Manuscript under review for journal Atmos. Chem. Phys.
Discussion started: 2 March 2017

We compared MIPAS CCl_4 profiles to profiles derived from the balloon version of MIPAS (MIPAS-B) and from the solar occultation ACE-FTS instrument. While MIPAS-B validation covers both FR and OR mission phases at selected latitudes, ACE validation covers the OR phase, globally, for latitudes larger than 45 degrees. In general, MIPAS/ENVISAT measurements are within 10% of both instruments for pressures between 100 and 40 hPa. A positive bias is found mainly in tropical regions at very low altitudes for OR measurements. In the latitude band 50S-70S, MIPAS shows a larger negative bias with respect to ACE-FTS, but this bias seems to reduce when compared with the upcoming version of ACE-FTS products. For pressures smaller than 40 hPa, MIPAS/ENVISAT CCl_4 values are between MIPAS-B and ACE-FTS.

We used the CCl_4 measurements to estimate for the first time the CCl_4 trends as a function of both latitude and pressure, including the photolytic loss region (70-20 hPa). Negative trends ($-10/-15$ pptv/decade, $-10/-30$ %/decade) are observed at all latitudes in the UTLS region, with the exception of slightly positive values ($5/10$ pptv/decade, $15/20$ %/decade) for a limited region at Southern mid-latitudes between 50 and 10 hPa. In general, CCl_4 VMR values exhibit a smaller decline rate for the SH than the NH. The magnitude of the negative trend increases with altitude, more strongly in the NH, reaching values of 30-35%/decade at 50 hPa, close to the lifetime limited rate. The hemispheric asymmetry of the trend is probably related to the asymmetry in the general circulation of the atmosphere.

An approach based on tracer-tracer linear correlations was used to estimate CCl_4 atmospheric lifetime in the lower stratosphere. The calculation provides a global average lifetime of 46(38 - 60) years considering CFC-11 as reference tracer and 48(41 - 58) years considering CFC-12. These results are consistent with the most recent literature results of 44(36 - 58) years (SPARC, 2013, 2016). We also computed the CCl_4 lifetime separately for the two hemispheres. For the NH we obtain 47(39 - 61) years considering CFC-11 as reference and 47(41 - 56) years considering CFC-12 as reference. For the SH we obtain 45(38 - 59) years considering CFC-11 as reference and 49(42 - 59) years considering CFC-12.

8 Data availability

MIPAS ESA Level 2 products Version 7 can be obtained via https://earth.esa.int/web/guest/data-access (registration required). Trend values and related errors used to build the maps of Fig. 4 are available upon request to the authors.

Aknowledgements

We thank AGAGE leaders R. Prinn, R.Weiss, P. Krummel and S. O'Doherty for providing AGAGE data. AGAGE is supported principally by NASA (USA) grants to MIT and Scripps Institution of Oceanography, and also by DECC (UK) and NOAA (USA) grants to Bristol University and by CSIRO and BoM (Australia). Funding for the Atmospheric Chemistry Experiment was supplied primarily by the Canadian Space Agency.

References

Allen, N. D. C., Bernath, P. F., Boone, C. D., Chipperfield, M. P., Fu, D., Manney, G. L., Oram, D. E., Toon, G. C., and Weisenstein, D. K.: Global carbon tetrachloride distributions obtained from the Atmospheric Chemistry Experiment (ACE), Atmospheric Chemistry and Physics, 9, 7449–7459, doi:10.5194/acp-9-7449-2009, http://www.atmos-chem-phys.net/9/7449/2009/, 2009.

Bernath, P. F., McElroy, C. T., Abrams, M. C., Boone, C. D., Butler, M., Camy-Peyret, C., Carleer, M., Clerbaux, C., Coheur, P.-F., Colin, R., DeCola, P., DeMazière, M., Drummond, J. R., Dufour, D., Evans, W. F. J., Fast, H., Fussen, D., Gilbert, K., Jennings, D. E., Llewellyn, E. J., Lowe, R. P., Mahieu, E., McConnell, J. C., McHugh, M., McLeod, S. D., Michaud, R., Midwinter, C., Nassar, R., Nichitiu, F., Nowlan, C., Rinsland, C. P., Rochon, Y. J., Rowlands, N., Semeniuk, K., Simon, P., Skelton, R., Sloan, J. J., Soucy, M.-A., Strong, K., Tremblay, P., Turnbull, D., Walker, K. A., Walkty, I., Wardle, D. A., Wehrle, V., Zander, R., and Zou, J.: Atmospheric Chemistry Experiment (ACE): Mission overview, Geophysical Research Letters, 32, doi:10.1029/2005GL022386, http://dx.doi.org/10.1029/2005GL022386, l15S01, 2005.

Boone, C. D., Nassar, R., Walker, K. A., Rochon, Y., McLeod, S. D., Rinsland, C. P., and Bernath, P. F.: Retrievals for the atmospheric chemistry experiment Fourier-transform spectrometer, Appl. Opt., 44, 7218–7231, doi:10.1364/AO.44.007218, http://ao.osa.org/abstract.cfm?URI=ao-44-33-7218, 2005.

Boone, C. D., Walker, K. A., and Bernath, P. F.: Version 3 retrievals for the atmospheric chemistry experiment Fourier transform spectrometer (ACE-FTS), The Atmospheric Chemistry Experiment ACE at, 10, 103–127, 2013.

Brown, A. T., Chipperfield, M. P., Boone, C., Wilson, C., Walker, K. A., and Bernath, P. F.: Trends in atmospheric halogen containing gases since 2004, Journal of Quantitative Spectroscopy and Radiative Transfer, 112, 2552 – 2566, doi:http://dx.doi.org/10.1016/j.jqsrt.2011.07.005, http://www.sciencedirect.com/science/article/pii/S0022407311002706, 2011.

Brown, A. T., Volk, C. M., Schoeberl, M. R., Boone, C. D., and Bernath, P. F.: Stratospheric lifetimes of CFC-12, CCl4, CH4, CH3Cl and N2O from measurements made by the Atmospheric Chemistry Experiment-Fourier Transform Spectrometer (ACE-FTS), Atmospheric Chemistry and Physics, 13, 6921–6950, doi:10.5194/acp-13-6921-2013, http://www.atmos-chem-phys.net/13/6921/2013/, 2013.

Butler, J. H., Yvon-Lewis, S. A., Lobert, J. M., King, D. B., Montzka, S. A., Bullister, J. L., Koropalov, V., Elkins, J. W., Hall, B. D., Hu, L., and Liu, Y.: A comprehensive estimate for loss of atmospheric carbon tetrachloride (CCl_4) to the ocean, Atmospheric Chemistry and Physics, 16, 10 899–10 910, doi:10.5194/acp-16-10899-2016, http://www.atmos-chem-phys.net/16/10899/2016/, 2016.

Carpenter, L., Reimann, S., Burkholder, J., Clerbaux, C., Hall, B., Hossaini, R., Laube, J., and Yvon-Lewis, S.: Update on Ozone-Depleting Substances (ODSs) and Other Gases of Interest to the Montreal Protocol, in: Scientific Assessment of Ozone Depletion: 2014, edited by Research, G. O. and Monitoring Project, R. N. ., chap. 1, World Meteorological Organization, Geneva, Switzerland, 2014.

Castelli, E., Ridolfi, M., Carlotti, M., Sinnhuber, B.-M., Kirner, O., Kiefer, M., and Dinelli, B. M.: Errors induced by different approximations in handling horizontal atmospheric inhomogeneities in MIPAS/ENVISAT retrievals, Atmospheric Measurement Techniques, 9, 5499–5508, doi:10.5194/amt-9-5499-2016, http://www.atmos-meas-tech.net/9/5499/2016/, 2016.

Ceccherini, S.: Analytical determination of the regularization parameter in the retrieval of atmospheric vertical profiles, Opt. Lett., 30, 2554–2556, doi:10.1364/OL.30.002554, http://ol.osa.org/abstract.cfm?URI=ol-30-19-2554, 2005.

Ceccherini, S. and Ridolfi, M.: Technical Note: Variance-covariance matrix and averaging kernels for the Levenberg-Marquardt solution of the retrieval of atmospheric vertical profiles, Atmospheric Chemistry and Physics, 10, 3131–3139, doi:10.5194/acp-10-3131-2010, http://www.atmos-chem-phys.net/10/3131/2010/, 2010.

Ceccherini, S., Belotti, C., Carli, B., Raspollini, P., and Ridolfi, M.: Technical Note: Regularization performances with the error consistency method in the case of retrieved atmospheric profiles, Atmospheric Chemistry and Physics, 7, 1435–1440, doi:10.5194/acp-7-1435-2007, http://www.atmos-chem-phys.net/7/1435/2007/, 2007.

Chirkov, M., Stiller, G. P., Laeng, A., Kellmann, S., von Clarmann, T., Boone, C. D., Elkins, J. W., Engel, A., Glatthor, N., Grabowski, U., Harth, C. M., Kiefer, M., Kolonjari, F., Krummel, P. B., Linden, A., Lunder, C. R., Miller, B. R., Montzka, S. A., Mühle, J., O'Doherty, S., Orphal, J., Prinn, R. G., Toon, G., Vollmer, M. K., Walker, K. A., Weiss, R. F., Wiegele, A., and Young, D.: Global HCFC-22 measurements with MIPAS: retrieval, validation, global distribution and its evolution over 2005–2012, Atmospheric Chemistry and Physics, 16, 3345–3368, doi:10.5194/acp-16-3345-2016, http://www.atmos-chem-phys.net/16/3345/2016/, 2016.

Dudhia, A., Jay, V. L., and Rodgers, C. D.: Microwindow selection for high-spectral-resolution sounders, Appl. Opt., 41, 3665–3673, doi:10.1364/AO.41.003665, http://ao.osa.org/abstract.cfm?URI=ao-41-18-3665, 2002.

Eckert, E., von Clarmann, T., Kiefer, M., Stiller, G. P., Lossow, S., Glatthor, N., Degenstein, D. A., Froidevaux, L., Godin-Beekmann, S., Leblanc, T., McDermid, S., Pastel, M., Steinbrecht, W., Swart, D. P. J., Walker, K. A., and Bernath, P. F.: Drift-corrected trends and periodic variations in MIPAS IMK/IAA ozone measurements, Atmospheric Chemistry and Physics, 14, 2571–2589, doi:10.5194/acp-14-2571-2014, http://www.atmos-chem-phys.net/14/2571/2014/, 2014.

Eckert, E., Laeng, A., Lossow, S., Kellmann, S., Stiller, G., von Clarmann, T., Glatthor, N., Höpfner, M., Kiefer, M., Oelhaf, H., Orphal, J., Funke, B., Grabowski, U., Haenel, F., Linden, A., Wetzel, G., Woiwode, W., Bernath, P. F., Boone, C., Dutton, G. S., Elkins, J. W., Engel, A., Gille, J. C., Kolonjari, F., Sugita, T., Toon, G. C., and Walker, K. A.: MIPAS IMK/IAA CFC-11 (CCl_3F) and CFC-12 (CCl_2F_2) measurements: accuracy, precision and long-term stability, Atmospheric Measurement Techniques, 9, 3355–3389, doi:10.5194/amt-9-3355-2016, http://www.atmos-meas-tech.net/9/3355/2016/, 2016.

ESA: MIPAS readme file v7, https://earth.esa.int/web/sppa/mission-performance/esa-missions/envisat/mipas/products-and-algorithms/products-information/, lastchecked on 2016-09-19, 2016.

Fischer, H., Birk, M., Blom, C., Carli, B., Carlotti, M., von Clarmann, T., Delbouille, L., Dudhia, A., Ehhalt, D., Endemann, M., Flaud, J. M., Gessner, R., Kleinert, A., Koopman, R., Langen, J., López-Puertas, M., Mosner, P., Nett, H., Oelhaf, H., Perron, G., Remedios, J., Ridolfi, M., Stiller, G., and Zander, R.: MIPAS: an instrument for atmospheric and climate research, Atmospheric Chemistry and Physics, 8, 2151–2188, doi:10.5194/acp-8-2151-2008, http://www.atmos-chem-phys.net/8/2151/2008/, 2008.

Friedl-Vallon, F., Maucher, G., Seefeldner, M., Trieschmann, O., Kleinert, A., Lengel, A., Keim, C., Oelhaf, H., and Fischer, H.: Design and characterization of the balloon-borne Michelson Interferometer for Passive Atmospheric Sounding (MIPAS-B2), Appl. Opt., 43, 3335–3355, doi:10.1364/AO.43.003335, http://ao.osa.org/abstract.cfm?URI=ao-43-16-3335, 2004.

Graziosi, F., Arduini, J., Bonasoni, P., Furlani, F., Giostra, U., Manning, A. J., McCulloch, A., O'Doherty, S., Simmonds, P. G., Reimann, S., Vollmer, M. K., and Maione, M.: Emissions of Carbon Tetrachloride (CCl_4) from Europe, Atmospheric Chemistry and Physics Discussions, 2016, 1–24, doi:10.5194/acp-2016-326, http://www.atmos-chem-phys-discuss.net/acp-2016-326/, 2016.

Harris, N., Wuebbles, D., Daniel, J., Hu, J., Kuijpers, L., Law, K., Prather, M., and Schofield, R.: Scenarios and information for policy makers, in: Scientific Assessment of Ozone Depletion: 2014, edited by Research, G. O. and Monitoring Project, R. N. ., chap. 5, World Meteorological Organization, Geneva, Switzerland, 2014.

Hegglin, M. and Tegtmeier, S.: The SPARC Data Initiative, SPARC Newsletter, 36, 22–23, 2011.

Höpfner, M., Oelhaf, H., Wetzel, G., Friedl-Vallon, F., Kleinert, A., Lengel, A., Maucher, G., Nordmeyer, H., Glatthor, N., Stiller, G., Clarmann, T. v., Fischer, H., Kröger, C., and Deshler, T.: Evidence of scattering of tropospheric radiation by PSCs in mid-IR limb emission

spectra: MIPAS-B observations and KOPRA simulations, Geophysical Research Letters, 29, 119–1–119–4, doi:10.1029/2001GL014443, http://dx.doi.org/10.1029/2001GL014443, 2002.

Kellmann, S., von Clarmann, T., Stiller, G. P., Eckert, E., Glatthor, N., Höpfner, M., Kiefer, M., Orphal, J., Funke, B., Grabowski, U., Linden, A., Dutton, G. S., and Elkins, J. W.: Global CFC-11 (CCl_3F) and CFC-12 (CCl_2F_2) measurements with the Michelson Interferometer for Passive Atmospheric Sounding (MIPAS): retrieval, climatologies and trends, Atmospheric Chemistry and Physics, 12, 11 857–11 875, doi:10.5194/acp-12-11857-2012, http://www.atmos-chem-phys.net/12/11857/2012/, 2012.

Kleinert, A., Aubertin, G., Perron, G., Birk, M., Wagner, G., Hase, F., Nett, H., and Poulin, R.: MIPAS Level 1B algorithms overview: operational processing and characterization, Atmospheric Chemistry and Physics, 7, 1395–1406, doi:10.5194/acp-7-1395-2007, http://www.atmos-chem-phys.net/7/1395/2007/, 2007.

Kyrölä, E., Tamminen, J., Sofieva, V., Bertaux, J. L., Hauchecorne, A., Dalaudier, F., Fussen, D., Vanhellemont, F., Fanton d'Andon, O., Barrot, G., Guirlet, M., Fehr, T., and Saavedra de Miguel, L.: GOMOS O_3, NO_2, and NO_3 observations in 2002–2008, Atmospheric Chemistry and Physics, 10, 7723–7738, doi:10.5194/acp-10-7723-2010, http://www.atmos-chem-phys.net/10/7723/2010/, 2010.

Liang, Q., Newman, P. A., Daniel, J. S., Reimann, S., Hall, B. D., Dutton, G., and Kuijpers, L. J. M.: Constraining the carbon tetrachloride (CCl4) budget using its global trend and inter-hemispheric gradient, Geophysical Research Letters, 41, 5307–5315, doi:10.1002/2014GL060754, http://dx.doi.org/10.1002/2014GL060754, 2014GL060754, 2014.

Lovelock, J. E., Maggs, R. J., and Wade, R. J.: Halogenated Hydrocarbons in and over the Atlantic, Nature, 241, 194–196, doi:http://dx.doi.org/10.1038/241194a0, 1973.

Montzka, S. A., Butler, J. H., Elkins, J., Thompson, T. M., Clarke, A. D., and Lock, L. T.: Present and future trends in the atmospheric burden of ozone-depleting halogens, Nature, 398, 690–694, doi:http://dx.doi.org/10.1038/19499, 1999.

Naujokat, B. and Grunow, K.: The stratospheric Arctic winter 2002/03: balloon flight planning by trajectory calculations, in: Proceedings of the 16th ESA Symposium on European Rocket and Balloon Programmes and Related Research, pp. 421–425, ESA SP-530, St. Gallen, 2003.

Oxford University: MIPAS website, http://eodg.atm.ox.ac.uk/MIPAS/, lastchecked on 2016-09-19, 2016.

Perrin, A., Flaud, J.-M., Ridolfi, M., VanderÂ Auwera, J., and Carlotti, M.: MIPAS database: new HNO_3 line parameters at 7.6 µm validated with MIPAS satellite measurements, Atmospheric Measurement Techniques, 9, 2067–2076, doi:10.5194/amt-9-2067-2016, http://www.atmos-meas-tech.net/9/2067/2016/, 2016.

Plumb, R. A.: Tracer interrelationships in the stratosphere, Reviews of Geophysics, 45, n/a–n/a, doi:10.1029/2005RG000179, http://dx.doi.org/10.1029/2005RG000179, rG4005, 2007.

Plumb, R. A. and Ko, M. K. W.: Interrelationships between mixing ratios of long-lived stratospheric constituents, Journal of Geophysical Research: Atmospheres, 97, 10 145–10 156, doi:10.1029/92JD00450, http://dx.doi.org/10.1029/92JD00450, 1992.

Prinn, R., Weiss, R., P.J., F., Simmonds, P., Cunnold, D., O'Doherty, S., Salameh, P., Porter, L., Krummel, P., Wang, R. H., Miller, B., Harth, C., Greally, B., Van Woy, F., Steele, L., Mühle, J., Sturrock, G., Alyea, F., Huang, J., and Hartley, D.: The ALE / GAGE AGAGE Network, Carbon Dioxide Information Analysis Center (CDIAC), Oak Ridge National Laboratory (ORNL), U.S. Department of Energy (DOE), 2016.

Prinn, R. G., Weiss, R. F., Fraser, P. J., Simmonds, P. G., Cunnold, D. M., Alyea, F. N., O'Doherty, S., Salameh, P., Miller, B. R., Huang, J., Wang, R. H. J., Hartley, D. E., Harth, C., Steele, L. P., Sturrock, G., Midgley, P. M., and McCulloch, A.: A history of chemically and radiatively important gases in air deduced from ALE/GAGE/AGAGE, Journal of Geophysical Research: Atmospheres, 105, 17 751–17 792, doi:10.1029/2000JD900141, http://dx.doi.org/10.1029/2000JD900141, 2000.

Raspollini, P., Carli, B., Carlotti, M., Ceccherini, S., Dehn, A., Dinelli, B. M., Dudhia, A., Flaud, J.-M., López-Puertas, M., Niro, F., Remedios, J. J., Ridolfi, M., Sembhi, H., Sgheri, L., and von Clarmann, T.: Ten years of MIPAS measurements with ESA Level 2 processor V6; Part 1: Retrieval algorithm and diagnostics of the products, Atmospheric Measurement Techniques, 6, 2419–2439, doi:10.5194/amt-6-2419-2013, http://www.atmos-meas-tech.net/6/2419/2013/, 2013.

Rhew, R. C. and Happell, J. D.: The atmospheric partial lifetime of carbon tetrachloride with respect to the global soil sink, Geophysical Research Letters, 43, 2889–2895, doi:10.1002/2016GL067839, http://dx.doi.org/10.1002/2016GL067839, 2016GL067839, 2016.

Ridolfi, M. and Sgheri, L.: A self-adapting and altitude-dependent regularization method for atmospheric profile retrievals, Atmospheric Chemistry and Physics, 9, 1883–1897, doi:10.5194/acp-9-1883-2009, http://www.atmos-chem-phys.net/9/1883/2009/, 2009.

Ridolfi, M. and Sgheri, L.: Iterative approach to self-adapting and altitude-dependent regularization for atmospheric profile retrievals, Opt. Express, 19, 26 696–26 709, doi:10.1364/OE.19.026696, http://www.opticsexpress.org/abstract.cfm?URI=oe-19-27-26696, 2011.

Rinsland, C. P., Mahieu, E., Demoulin, P., Zander, R., Servais, C., and Hartmann, J.-M.: Decrease of the carbon tetrachloride (CCl4) loading above Jungfraujoch, based on high resolution infrared solar spectra recorded between 1999 and 2011, Journal of Quantitative Spectroscopy and Radiative Transfer, 113, 1322 – 1329, doi:http://dx.doi.org/10.1016/j.jqsrt.2012.02.016, http://www.sciencedirect.com/science/article/pii/S0022407312000763, three Leaders in Spectroscopy, 2012.

Rothman, L., Jacquemart, D., Barbe, A., Benner, D. C., Birk, M., Brown, L., Carleer, M., Jr., C. C., Chance, K., Coudert, L., Dana, V., Devi, V., Flaud, J.-M., Gamache, R., Goldman, A., Hartmann, J.-M., Jucks, K., Maki, A., Mandin, J.-Y., Massie, S., Orphal, J., Perrin, A., Rinsland, C., Smith, M., Tennyson, J., Tolchenov, R., Toth, R., Auwera, J. V., Varanasi, P., and Wagner, G.: The {HITRAN} 2004 molecular spectroscopic database, Journal of Quantitative Spectroscopy and Radiative Transfer, 96, 139 – 204, doi:http://dx.doi.org/10.1016/j.jqsrt.2004.10.008, http://www.sciencedirect.com/science/article/pii/S0022407305001081, 2005.

Rothman, L., Gordon, I., Barbe, A., Benner, D., Bernath, P., Birk, M., Boudon, V., Brown, L., Campargue, A., Champion, J.-P., Chance, K., Coudert, L., Dana, V., Devi, V., Fally, S., Flaud, J.-M., Gamache, R., Goldman, A., Jacquemart, D., Kleiner, I., Lacome, N., Lafferty, W., Mandin, J.-Y., Massie, S., Mikhailenko, S., Miller, C., Moazzen-Ahmadi, N., Naumenko, O., Nikitin, A., Orphal, J., Perevalov, V., Perrin, A., Predoi-Cross, A., Rinsland, C., Rotger, M., Šimečková, M., Smith, M., Sung, K., Tashkun, S., Tennyson, J., Toth, R., Vandaele, A., and Auwera, J. V.: The HITRAN 2008 molecular spectroscopic database, Journal of Quantitative Spectroscopy and Radiative Transfer, 110, 533 – 572, doi:http://dx.doi.org/10.1016/j.jqsrt.2009.02.013, http://www.sciencedirect.com/science/article/pii/S0022407309000727, 2009.

Sheese, P. E., Boone, C. D., and Walker, K. A.: Detecting physically unrealistic outliers in ACE-FTS atmospheric measurements, Atmospheric Measurement Techniques, 8, 741–750, doi:10.5194/amt-8-741-2015, http://www.atmos-meas-tech.net/8/741/2015/, 2015.

Simmonds, P., Cunnold, D., Alyea, F., Cardelino, C., Crawford, A., Prinn, R., Fraser, P., Rasmussen, R., and Rosen, R.: Carbon tetrachloride lifetimes and emissions determined from daily global measurements during 1978–1985, Journal of atmospheric chemistry, 7, 35–58, 1988.

Simmonds, P. G., Cunnold, D. M., Weiss, R. F., Prinn, R. G., Fraser, P. J., McCulloch, A., Alyea, F. N., and O'Doherty, S.: Global trends and emission estimates of CCl4 from in situ background observations from July 1978 to June 1996, Journal of Geophysical Research: Atmospheres, 103, 16 017–16 027, doi:10.1029/98JD01022, http://dx.doi.org/10.1029/98JD01022, 1998.

Singh, H. B., Fowler, D. P., and Peyton, T. O.: Atmospheric Carbon Tetrachloride: Another Man-Made Pollutant, Science, 192, 1231–1234, doi:10.1126/science.192.4245.1231, http://science.sciencemag.org/content/192/4245/1231, 1976.

SPARC: SPARC Report on the Lifetimes of Stratospheric Ozone-Deleting Substances, Their Replacements, and Related Species, M.K.W. Ko, P.A. Newman, S. Reimann, S.E. Strahan (eds.), available at www.sparc-climate.org/publications/sparc-reports/sparc-report-no6, 2013.

SPARC: SPARC Report on the Mystery of Carbon tetrachloride, SPARC Report No. 7, WCRP-13/2016. Liang Q. and Newman P.A. and S. Reimann (eds.), available at: www.sparc-climate.org/publications/sparc-reports/sparc-report-no7, 2016.

Stiller, G., Clarmann, T. v., Haenel, F., Funke, B., Glatthor, N., Grabowski, U., Kellmann, S., Kiefer, M., Linden, A., Lossow, S., et al.: Observed temporal evolution of global mean age of stratospheric air for the 2002 to 2010 period, Atmospheric Chemistry and Physics, 12, 3311–3331, 2012.

Stiller, G. P., von Clarmann, T., Funke, B., Glatthor, N., Hase, F., Höpfner, M., and Linden, A.: Sensitivity of trace gas abundances retrievals from infrared limb emission spectra to simplifying approximations in radiative transfer modelling, Journal of Quantitative Spectroscopy and Radiative Transfer, 72, 249 – 280, doi:http://dx.doi.org/10.1016/S0022-4073(01)00123-6, http://www.sciencedirect.com/science/article/pii/S0022407301001236, 2002.

Volk, C. M., Elkins, J. W., Fahey, D. W., Dutton, G. S., Gilligan, J. M., Loewenstein, M., Podolske, J. R., Chan, K. R., and Gunson, M. R.: Evaluation of source gas lifetimes from stratospheric observations, Journal of Geophysical Research: Atmospheres, 102, 25 543–25 564, doi:10.1029/97JD02215, http://dx.doi.org/10.1029/97JD02215, 1997.

Wetzel, G., Oelhaf, H., Kirner, O., Friedl-Vallon, F., Ruhnke, R., Ebersoldt, A., Kleinert, A., Maucher, G., Nordmeyer, H., and Orphal, J.: Diurnal variations of reactive chlorine and nitrogen oxides observed by MIPAS-B inside the January 2010 Arctic vortex, Atmospheric Chemistry and Physics, 12, 6581–6592, doi:10.5194/acp-12-6581-2012, http://www.atmos-chem-phys.net/12/6581/2012/, 2012.

World Meteorological Organization (WMO): Scientific Assessment of Ozone Depletion: 1998, Geneva, Switzerland, 1999.

World Meteorological Organization (WMO): Scientific Assessment of Ozone Depletion: 2010, Global Ozone Research and Monitoring Project - Report No. 52, Geneva, Switzerland, 516 pp., 2011.